Nucleic Acids Research, 2025, **53**, gkaf125
https://doi.org/10.1093/nar/gkaf125
Gene regulation, Chromatin and Epigenetics

A noncanonical intrinsic terminator in the HicAB toxin–antitoxin operon promotes the transmission of conjugative antibiotic resistance plasmids

Jianzhong Lin[1,2,†], **Songwei Ni**[1,3,†], **Baiyuan Li**[4,†], **Yunxue Guo**[1,2,3,†], **Xinyu Gao**[1,2], **Yabo Liu**[1,3], **Lingxian Yi**[5], **Pengxia Wang**[1,2,3], **Ran Chen**[1,3], **Jianyun Yao**[1,3], **Thomas K. Wood**[6], **Xiaoxue Wang**[1,2,3,*]

[1]Key Laboratory of Tropical Oceanography, Key Laboratory of Tropical Marine Bio-resources and Ecology, South China Sea Institute of Oceanology, Chinese Academy of Sciences, No.1119, Haibin Road, Nansha District, Guangzhou 511458, China
[2]University of Chinese Academy of Sciences, Beijing 100049, China
[3]Southern Marine Science and Engineering Guangdong Laboratory (Guangzhou), No.1119, Haibin Road, Nansha District, Guangzhou 511458, China
[4]Key Laboratory of Comprehensive Utilization of Advantage Plants Resources in Hunan South, College of Chemistry and Bioengineering, Hunan University of Science and Engineering, Yongzhou 425199 Hunan, China
[5]Fujian Key Laboratory of Traditional Chinese Veterinary Medicine and Animal Health, College of Animal Sciences (College of Bee Science), Fujian Agriculture and Forestry University, Fuzhou 350002, China
[6]Department of Chemical Engineering, Pennsylvania State University, University Park, PA 16802-4400, United States

[*]To whom correspondence should be addressed. Email: xxwang@scsio.ac.cn
[†]The first four authors should be regarded as Joint First Authors.

Abstract

Conjugative plasmids, major vehicles for the spread of antibiotic resistance genes, often contain multiple toxin–antitoxin (TA) systems. However, the physiological functions of TA systems remain obscure. By studying two TA families commonly found on colistin-resistant IncI2 *mcr-1*-bearing plasmids, we discovered that the HicAB TA, rather than the StbDE TA, acts as a crucial addiction module to increase horizontal plasmid–plasmid competition. In contrast to the canonical type II TA systems in which the TA genes are cotranscribed and/or the antitoxin gene has an additional promoter to allow for an increased antitoxin/toxin ratio, the HicAB TA system with the toxin gene preceding the antitoxin gene employs internal transcription termination to allow for a higher toxin production. This intrinsic terminator, featuring a G/C-rich hairpin with a UUU tract, lies upstream of the antitoxin gene, introducing a unique mechanism for the enhancing toxin/antitoxin ratio. Critically, the *hicAB* TA significantly contributes to plasmid competition and plasmid persistence in the absence of antibiotic selection, and deleting this intrinsic terminator alone diminishes this function. These findings align with the observed high occurrence of *hicAB* in IncI2 plasmids and the persistence of these plasmids after banning colistin as a feed additive. This study reveals how reprogramming the regulatory circuits of TA operons impacts plasmid occupancy in the microbial community and provides critical targets for combating antibiotic resistance.

Graphical abstract

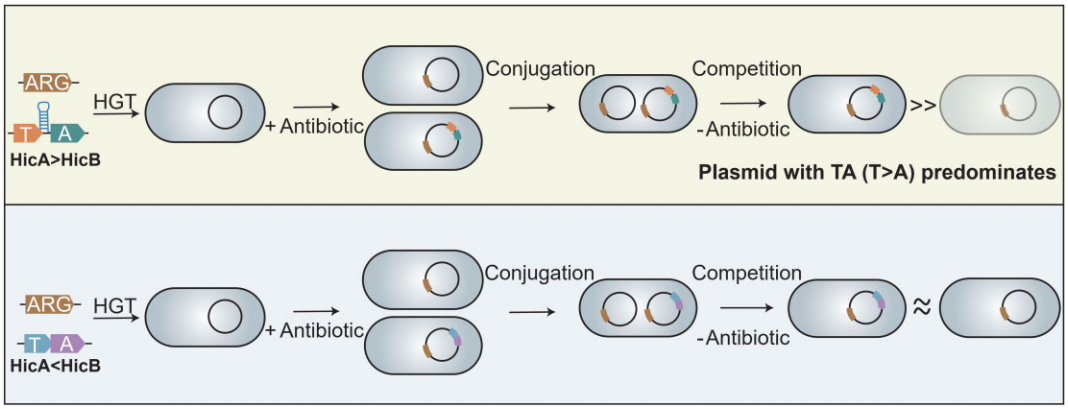

Received: October 24, 2024. **Revised:** January 24, 2025. **Editorial Decision:** February 5, 2025. **Accepted:** February 10, 2025

Introduction

Toxin–antitoxin (TA) systems, including CcdB/CcdA of the F plasmid [1, 2] and Hok/Sok and Kis/Kid (encoded by the ParD operon) of the R1 plasmid [3, 4], were first discovered on conjugative plasmids in the 1980s. Comprising two primary components, TA systems consist of a toxin capable of disrupting essential cellular processes and an antitoxin that counters the activity of the toxin [5]. TA systems are prevalent in the chromosomes of bacteria and archaea, as well as in mobile genetic elements such as plasmids and phages [6, 7]. They play roles in maintaining mobile genetic elements [8, 9], biofilm formation and stress responses [10], and mediating phage resistance. Toxins in TA systems target essential cellular processes such as cell division, transcription, and translation or disrupt membrane integrity [6, 11]. In most cases, toxin activity is strictly controlled at the transcriptional, translational, or post-translational modification level to prevent excessive toxin expression [12, 13]. Toxin activation can occur in biofilms [14] or during phage attacks [15, 16] to interfere with normal cellular function, and the way in which the antitoxin neutralizes the toxin is of special interest in the TA field, as it reflects the way in which the toxin is liberated from the inhibition of the antitoxin. On the basis of the ability of the antitoxins to neutralize the toxic effects of the toxins, TA systems are currently categorized into eight types (types I–VIII) [6, 11]. Antitoxin, either as a non-coding RNA or a protein, directly or indirectly interacts with the toxin or its target to prevent the activity of the toxin [6]. Among the eight types of TA systems, type II TA systems are the most extensively studied, in which the antitoxin protein directly binds the toxin protein to neutralize the toxicity of the toxin. It has been traditionally believed that the activation of type II toxins largely relies on the degradation of the labile antitoxin by cellular proteases such as Lon, ClpXP, and ClpAP, and antitoxin degradation also leads to derepress of TA transcription [17–19]. However, although free antitoxins are less stable than the cognate toxins, studies have found antitoxins engaged in the TA complex can be protected from proteolysis and stress, and TA transcription activities have a limited impact on antitoxin stability [11, 20].

Plasmids carrying antibiotic resistance genes (ARGs) and virulence genes endow host bacteria with new adaptive traits, but they frequently impose a metabolic burden on the host [21, 22]. Thus, plasmid loss sometimes occurs in the absence of selection for plasmid-encoded traits [23]. Toxin-mediated killing of plasmid-free daughter cells due to segregation error was initially proposed as a model to explain the function of plasmid-encoded TA in reducing plasmid loss during vertical inheritance [1, 8, 24]. As one of the major vehicles of horizontal gene transfer, conjugative plasmids encode their own replication and segregation modules to ensure vertical inheritance [25, 26], and studies reported that deleting TA loci from conjugative plasmids did not affect plasmid stability [27–29]. Intriguingly, conjugative plasmids frequently encode multiple TA pairs, suggesting the function of each TA pair may go beyond maintaining plasmid vertical stability.

Horizontal transmission of plasmids between bacteria significantly influences plasmid persistence and inheritance within host populations. The 'competition hypothesis' proposes that TA systems are selected for plasmids due to their role in enhancing plasmid transmission during horizontal transfer [30]. This hypothesis is supported by studies demonstrating that the ParE/ParD TA system encoded by the pTP100 plasmid outcompetes TA-lacking plasmids during gene transfer events [30]. Despite the highly diversified TA systems found in various conjugative plasmids [31], clarifying the contributions of each TA family to vertical and horizontal plasmid transmission remains challenging due to the presence of multiple plasmid copies and TA systems per plasmid.

The emergence of the IncI2 plasmid-mediated colistin resistance gene *mcr-1* was reported in 2016, and it has spread to over 60 regions/countries, posing significant health risks [32–34]. MCR-1, a transmembrane protein, modifies lipid A with phosphoethanolamine (pEtN) in the periplasmic space, thereby conferring colistin resistance [35]. The expression of *mcr-1* comes with a fitness cost, and *mcr-1*-bearing plasmids typically maintain low copy numbers while exhibiting high conjugative potential across diverse Gram-negative bacteria [22, 34]. The global dissemination of *mcr-1* in China is largely attributed to the selective pressure exerted by the use of colistin in agriculture, particularly as a feed additive [36]. The distribution of *mcr-1* spans 20 types of plasmids, with IncX4, IncI2, and IncHI2 conjugative plasmids identified as the predominant plasmid replicon types [37, 38]. The IncX4 and IncI2 conjugative plasmids also carry other ARGs including bla_{KPC}, $bla_{\text{CTX-M-14b}}$ and $bla_{\text{CTX-M-55}}$, conferring resistance to beta-lactam antibiotics [39–41]. A 7-year surveillance study (2013–2019) revealed a rapid decline in the predominant IncX4 plasmids but only a slight decline in IncI2 plasmids after the ban on the use of colistin as a feed additive for animals was implemented in May 2017 in China [23, 34]. In particular, when genome sequencing was used to track associated changes in *mcr-1*-positive *Escherichia coli* samples from farmed animals, humans, food, and the environment of Guangzhou in a two-year timeframe, the diversity of *mcr-1*-associated plasmid types decreased, and the proportion of IncI2 plasmids relative to *mcr*-1-encoding plasmids significantly increased after the ban [42]. This persistence suggests that IncI2-type conjugative plasmids may have adapted to increase their transmission in the absence of external selection pressure.

Genomic analysis reveals various TA systems on *mcr-1*-bearing plasmids shared across IncI2 and IncX4 plasmids. Here, we investigated two TA families, HicAB and StbDE, which are commonly found on *mcr-1*-bearing IncI2 and IncX4 plasmids. Using the representative IncI2 plasmid pHNSHP45 (p45), we discovered that p45 plasmids lacking both TA systems were stably maintained in host cells, regardless of the retention or disruption of the horizontal transmission capability of the plasmid. These findings indicate that the HicAB and StbDE systems are dispensable in terms of maintaining the vertical stability of the p45 plasmid. Instead, we found that HicAB, rather than StbDE, plays a crucial role in mediating horizontal plasmid–plasmid competition. Surprisingly, a noncanonical intrinsic terminator inside the *hicAB* operons is predominantly present in IncI2 plasmids. This terminator increases the production of toxin relative to the antitoxin within the HicAB system, which is crucial for driving plasmid–plasmid competition and enhancing the transmission of *mcr-1*-bearing plasmids. Additionally, another subfamily of overlapping *hicAB* operons that lack this terminator, which is predominantly found in IncX4 plasmids, has almost no contribution to plasmid competitive advantage. Thus, the functional characterization across different type II TA families on stringent-control conjugative plasmids supports

a model where TAs drive horizontal competition through an imbalanced toxin/antitoxin ratio. This cooperative action also facilitates the spread of HicAB TA modules in microbial communities, underscoring the selfish nature of TA systems.

Materials and methods

Bacterial strains, plasmids, and growth conditions

Details of the bacterial strains, plasmids, and primers used can be found in Supplementary Tables S1 and S2. *Escherichia coli* strains were grown in Luria broth (LB) at 37°C, with the exception of strains carrying pKD46, which were cultured at 30°C. For the auxotrophic *E. coli* strain WM3064, 2,6-diamino-pimelic acid (50 μg/ml), was added. Ampicillin (Amp, 100 μg/ml) was used to maintain the pKD46-, pUT18C-, pUC19-, pETDuet-, and pBAD-based plasmids. Kanamycin (Kan, 50 μg/ml) was used to maintain the pKT25- and pET28b-based plasmids. Chloramphenicol (Cm, 30 μg/ml) was used to maintain the pCA24N- and pBBR1Cm-based plasmids and the p45Δ*hicAB* plasmid in *the E. coli* K-12/p45: p45Δ*hicAB* strain. For specific strains such as K-12/p45: p45Δ*stbDE*, K-12/p45Δ*stbDE*: p45Δ*hicAB*, K-12/p14EC007a: p14EC007aΔ$hicA^{O}B$, K-12/p45: p45Δ$hicA^{T}B$::*gfp*, K-12/p45Δ*hicA*: p45Δ$hicA^{T}B$::*gfp*, and K-12/p45ΔTer: p45Δ$hicA^{T}B$::*gfp*, a combination of Cm and Kan was applied for plasmid maintenance. Gentamicin (Gm, 30 μg/ml) was used to maintain pHGM01-based plasmids. For gene expression induction, isopropyl-*β*-D-thiogalactopyranoside (IPTG) (0.5 mM for protein purification) and *L*-arabinose (0.005%∼0.3%) were used as inducers.

Bioinformatic analysis

To search the PLSDB plasmid database (version 2023_11_03_v2) [43], the $hicA^{T}B$, *stbDE*, and *mcr-1* nucleotide sequences in the p45 plasmid and the $hicA^{O}B$ nucleotide sequence in pJIE143 were used as inputs, and the default values of minimal percentage identity and minimal query coverage were 60 and 90, respectively. All of the data retrieved from the PLSDB plasmid database using BLASTn were compiled in Dataset S1. Multiple protein sequence alignment was performed using Clustal Omega [44] and visualized with the ESPript 3.0 web server [45].

Protein purification

The HicB, HicAB, and StbDE were purified from *E. coli* BL21 (DE3) harboring the corresponding plasmids pET28b-*hicB*-His, pETDuet-His-*hicA*-*hicB* and pET28b-*stbDE*-His. In brief, overnight cultures were diluted to an OD_{600} of 0.1 in LB. Upon reaching an OD_{600} of 0.8, IPTG was added and cells were collected after 5 h of induction. Subsequent steps for protein extraction were carried out following previously established protocols [46]. Tricine–sodium dodecyl sulphate–polyacrylamide gel electrophoresis (SDS–PAGE) analysis was conducted according to a previously described protocol [47].

Bacterial two-hybrid assays

The bacterial two-hybrid (BACTH) assay is designed to study protein-protein interactions in a bacterial system [48]. The pKT25 and pUT18C plasmids, each carrying distinct target-cloned inserts, were co-transformed into *E. coli* BTH101 (cya − 99) competent cells. The cotransformed cells were plated on LB agar supplemented with Amp, Kan, IPTG, and X-gal and incubated at 30°C for 36 h. Positive controls included pKT25-*zip* (fused with a leucine zipper protein) and pUT18C-*zip* plasmids (Euromedex), whereas negative controls included pKT25 (lacking an insert) and pUT18C-*zip* plasmids.

Primer extension

Primer extension was used to identify the transcription start sites of the *hicAB* and *stbDE* operons. The procedures were the same as those described previously with modifications [49]. Total RNA was isolated from K-12/pUC19-based cells using a Bacteria RNAprep Pure Kit (Tiangen Biotech Co. Ltd., China) according to the manufacturer's instructions. Subsequently, 1 μl of Carboxyfluorescein (FAM)-labeled primer was mixed with 4 μg of RNA in a 20 μl reaction. The reaction was denatured at 70°C for 5 min, then incubated on ice for 20 min, followed by 58°C for 20 min, and a final extension at room temperature for 15 min. The mixture was then supplemented with 6 μl $MgCl_2$, 3 μl 10 × buffer, 3 μl deoxyribonucleoside triphosphates (dNTPs), 0.75 μl ribonuclease inhibitor, 1.5 μl Avian Myeloblastosis Virus (AMV) reverse transcriptase, and 15.75 μl RNA. The reaction was incubated at 42°C for 1.5 h. Products were analyzed on an ABI3730 DNA Analyzer (Applied Biosystems, Foster City, California, USA) and processed with GeneMapper 4.1 (version 4.1).

Plasmid conjugation frequency assays

The conjugation frequency of p45 and its derivatives was examined via a previously published method [22]. In brief, WM3064 or K-12 strains harboring these megaplasmids were used as donors, and Kan-resistant K-12 or Gm-resistant K-12 strains were used as recipients. Transconjugants were selectively cultured on LB agar plates supplemented with PB (4 μg/ml) in combination with either Kan (50 μg/ml) or Gm (30 μg/ml) as needed. Transfer frequencies were calculated as the number of transconjugants per donor.

Plasmid loss frequency assays

Overnight cultures of *E. coli* strains (K-12 or K-12::*kan*) carrying plasmid p45 or its derivatives (p45Δ*hicA*, p45: p45Δ*hicAB*, p45Δ*hicAB*, p45Δ*hicAB*::*gfp*, p45Δ*stbE*, p45Δ*stbDE*, p45Δ*hicAB*Δ*stbDE*, p45Δ*oriT*, p45Δ*hicAB*Δ*stbDE*Δ*oriT*) were inoculated into LB at a ratio of 1:1000 without antibiotics. The cultures were subsequently subjected to serial passaging every 20 generations (the *E. coli* generation time is ∼20 min) at a ratio of 1:1000 [50]. The cultures were simultaneously diluted 10-fold to test the presence of the plasmid on LB, LB with Cm (10 μg/ml), and LB with Polymyxin B (PB, 4 μg/ml). For p45Δ*hicAB*Δ*stbDE*, p45Δ*oriT*, and p45Δ*hicAB*Δ*stbDE*Δ*oriT*, the plasmid loss frequency assay lasted 480 generations. For plasmid stability of pCA24N-based plasmids, overnight K-12 cells carrying pCA24N were inoculated into fresh LB with Cm (G0) and without Cm (G80-G480). Cultures collected at different generations were simultaneously diluted by 10-fold serials to test plasmid presence on the LB or LB with Cm plates. Plates were imaged after incubation at 37°C for 16 h, and Colony Forming Units (CFUs) were determined.

Plasmid copy number quantification by quantitative polymerase chain reaction

Overnight cultures of the K-12 strain carrying p45 or TA mutant derivatives were diluted to an initial OD_{600} of ∼0.1. The cultures were then incubated at 200 rpm in a shaker incubator using 250 ml Erlenmeyer flasks filled with 25 ml of LB, ensuring ample growth in a nutrient-rich environment. Following incubation at 37°C for 6 h, the cultures reached an OD_{600} of ∼5. Total DNA was subsequently extracted using the TIANamp Bacteria DNA Kit (Tiangen, China) following the manufacturer's instructions. The levels of p45 plasmid DNA were assessed by amplifying the plasmid-encoded single-copy gene *repA* using the primer pair *repA*-qF/qR. Simultaneously, the DNA levels of the chromosomes in the same sample were quantified by targeting the chromosomally encoded single-copy *gapdh* gene.

Real-time quantitative reverse-transcription polymerase chain reaction

Total RNA was extracted from the *E. coli* strains K12/p45, K12/p45ΔTer, 14EC007, 14EC017, and 14EC033 via the Bacteria RNAprep Pure Kit (Tiangen Biotech Co. Ltd., Beijing, China) following the manufacturer's protocols. For the reverse transcription process, 200 ng of total RNA was used to synthesize complementary DNA (cDNA) with the A3500 Reverse Transcription System (Promega, Madison, WI). Subsequently, 50 ng of the synthesized cDNA was employed in quantitative reverse-transcription polymerase chain reaction assays, which were conducted using a SYBR Green reaction mixture on the Step One Real-Time PCR System (Applied Biosystems). The expression levels of the target genes were normalized to those of the *purA* gene.

Western blotting

To quantify HicB levels in the K-12/p45 and K-12/p45ΔTer strains, overnight cultures of K-12/pBBR1-$hicA^{T}B$-C^{FLAG} and K-12/pBBR1-$hicA^{\Delta Ter}B$-C^{FLAG} strains were diluted 1:100 in fresh LB supplemented with Cm. Cultures in the exponential growth phase (OD_{600} ∼3) were harvested, and the OD_{600} was measured and the cultures were diluted in LB to an OD_{600} of 1.0. Subsequently, equal volumes of bacterial cultures were mixed with SDS–PAGE protein loading buffer, boiled for protein denaturation, and subjected to tricine–SDS–PAGE analysis. Proteins were transferred onto PVDF membranes for Western blotting using primary antibodies against the Flag-tag and horseradish peroxidase-conjugated goat anti-mouse secondary antibodies, as previously described [27]. The expression levels of the anti-RNA polymerase beta antibody (RNAP) served as an internal control in all of the samples, with horseradish peroxidase-conjugated goat anti-rabbit antibody used as the secondary antibody.

β-Galactosidase activity assays

β-Galactosidase activity in strains harboring the pHGR01-*lacZ* plasmid was evaluated using the Miller assay as previously described [27], with absorbance measurements taken at 420 nm. For translation efficiency determination, overnight cultures of strains containing the *lacZ* reporter plasmids P_{hicA}-*lacZ*, P_{hicB}-*lacZ*, P_{stbD}-*lacZ*, and P_{stbE}-*lacZ* were diluted 1:100 in fresh LB supplemented with Cm. β-galactosidase activity was determined for cells collected at an OD_{600} of 1.5. To determine the promoter activity of *hicA and hicB* upon expression of *hicB* and *hicAB*, pUC19, pUC19-*hicB*, pUC19-*hicAB*, and pUC19-$hicA^{\Delta Ter}B$ were transformed into K-12 carrying the P_{hicA}-*lacZ* and P_{hicB}-*lacZ* reporter. These overnight cultures were diluted 1:100 in LB with Cm and Amp, and β-galactosidase activity was determined for cells collected at an OD_{600} of 1.5.

Growth and toxicity assays, targeted gene deletion of p45 plasmid, cloning genes into plasmids, strand-specific RNA sequencing analysis, next-generation sequencing analysis, MIC determination, swimming motility and biofilm assays, and phage defense detection methods are described in the Supplemental ethods.

Results

The HicAB and StbDE TA systems are enriched on IncI2-type *mcr-1*-bearing plasmids

Analysis of plasmids obtained from the PLSDB (version 2023_11_23_v2, containing 59 895 plasmid records) revealed the presence of *mcr-1* in various plasmid replicon types [43]. Among them, the highest prevalence was observed in IncI2 conjugative plasmids (Fig. 1A), which are medium-sized (∼55–80 kb) conjugative plasmids known to harbor important antimicrobial resistance genes [51]. The IncI2-type plasmid p45, the first reported plasmid to transfer the *mcr-1* gene, was selected for this study [32]. Plasmid p45 is maintained at one copy number by the critical replication regulation gene *pcnR* [22]. The TADB database predicted that p45 harbors two putative TA systems: HicAB and StbDE (Fig. 1B) [52]. Further analysis revealed that these two putative TA systems are widely distributed across various plasmids, with ∼3/4 of them carrying HicAB and ∼1/2 carrying StbDE in the IncI2 types of plasmids (Fig. 1C). HicA belongs to the COG1724 family and HicB comprises the HicB-like antitoxin of pfam15919 and the ribbon–helix–helix domain of COG0864, both of which share low amino acid identity (∼20%) with the HicAB TA from *E. coli* K-12. Toxin StbD is categorized within the COG2161 functional family, whereas antitoxin StbE belongs to COG2026 (RelE functional family) or pfam05016 (ParE toxin protein family). As these predicted TA systems share low similarity with previously characterized TA systems, the following assays were conducted to determine whether they are *bona fide* TA systems. Cell viability tests in *E. coli* K-12 BW25113 (hereafter referred to as K-12) showed that HicA functions as a toxin and Live/Dead staining indicated that HicA toxin is bacteriostatic, with HicB serving as the corresponding antitoxin, since HicA is toxic and HicB is able to reduce HicA toxicity (Fig. 1D and Supplementary Fig. S1A and B). Similarly, StbE acts as a toxin, and StbD functions as its corresponding antitoxin.

Interestingly, unlike the *stbDE* operon, we observed a low level of toxicity for overexpressing *hicAB* via a pBAD vector under the arabinose-inducible promoter P_{BAD}, indicating that the *hicAB* operon might produce an excess of toxin HicA (Fig. 1D). A pull-down assay, using HicA with an N-terminal hexa-histidine tag (His-tag) together with untagged HicB, confirmed that HicA and HicB form a complex *in vitro*. Using the same approach, StbD and StbE were also found to form a complex (Fig. 1E and F). Tricine–SDS–PAGE analysis demonstrated that the sizes of the proteins pulled down by HicA-His and StbE-His matched well with the theoretical sizes of

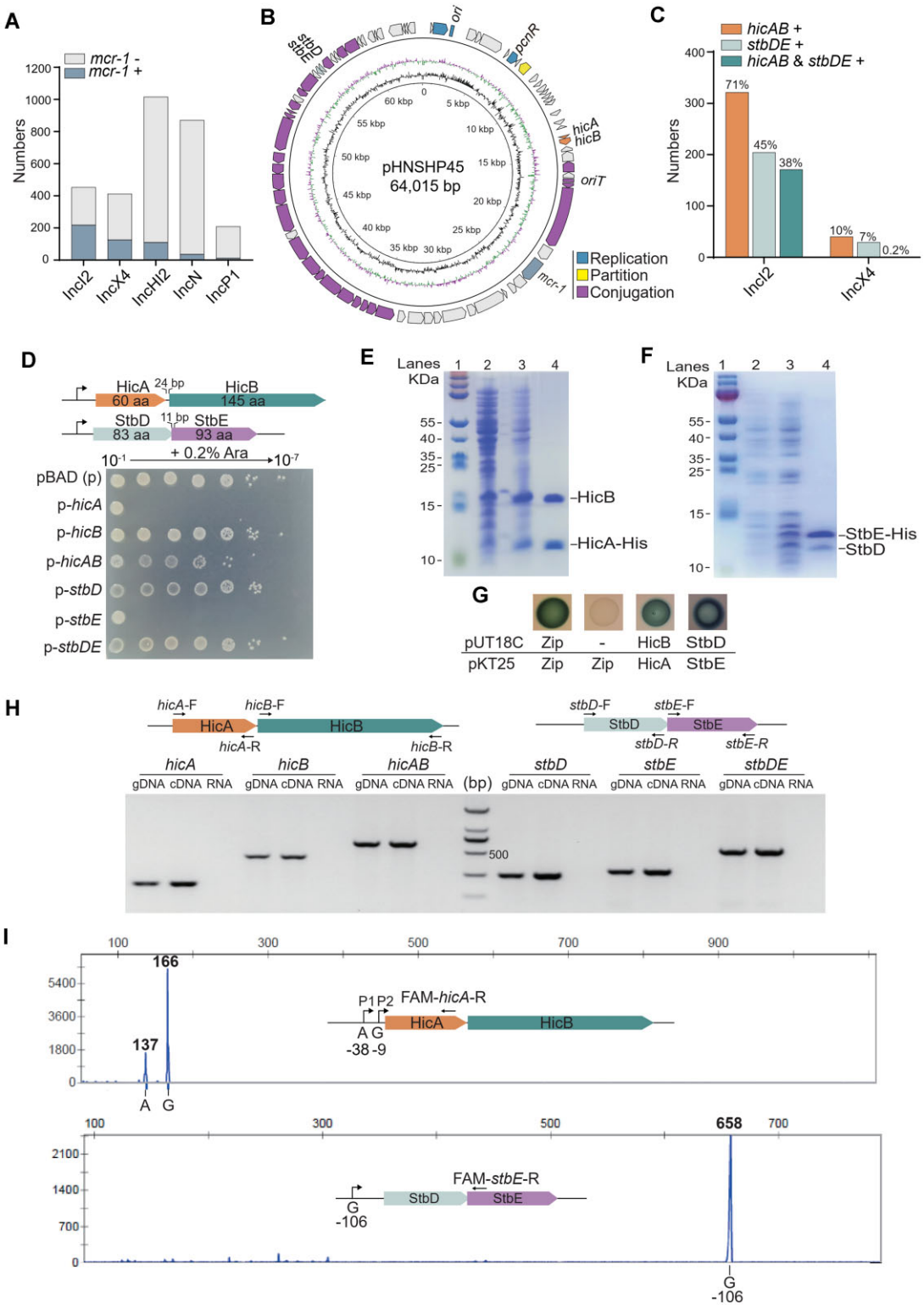

Figure 1. Type II HicAB and StbDE TAs are enriched on IncI2-type *mcr-1*-carrying plasmids. (**A**) The distribution and proportions of *mcr-1* in five primary types of plasmids were analyzed and retrieved from the PLSDB database. (**B**) Positions of *mcr-1*, the putative *hicAB,* and *stbDE* in pHNSHP45 (p45). (**C**) Distribution of two putative TA systems in IncI2 and IncX4 types of plasmids retrieved from the PLSDB database. (**D**) The organization of *hicAB* and *stbDE* TAs in p45 and toxicity test of each component and TA system in K-12 via pBAD (p) under the induction of 0.2% *L*-arabinose. (**E**) HicA and HicB form a complex *in vivo*. Lane 1: marker; Lane 2: negative control (NC, no IPTG); Lane 3: the HicAB complex was produced via pETDuet-His-*hicA*-*hicB* with a His-tag at the N-terminus in HicA; Lane 4: purified HicA^{T}B complex. (**F**) StbD and StbE form a complex *in vivo*, with StbD also forming protein dimers. Lane 1: marker; Lane 2: NC (no IPTG); Lane 3: the StbDE complex was produced via pET28b-*stbDE* with a His-tag at the C-terminal StbE; Lane 4: the purified StbDE complex. (**G**) The BACTH assay revealed that HicA interacts with HicB and that StbD interacts with StbE. Cells harboring pKT25-*zip* and pUT18C-*zip* plasmids were used as positive controls, and cells harboring pKT25 (without an insert) and pUT18C-*zip* plasmids were used as NCs. (**H**) Transcription analysis of *hicAB* and *stbDE*. gDNA: genomic DNA; cDNA: complementary DNA. (**I**) A primer extension assay using a 5′-FAM-labeled primer was conducted to identify the transcription initiation sites of the *hicAB* and *stbDE* TA operons. Representative images are shown in (D–H).

the HicB and StbD proteins, respectively. Cya-based bacterial two-hybrid (BACTH) assays confirmed a direct interaction between HicA and HicB, as well as between StbD and StbE (Fig. 1G). These assays confirmed that HicAB and StbDE are both type II TA systems.

HicAB and StbDE are both dispensable for vertical stability of the p45 plasmid

Plasmid-encoded TA systems were initially proposed to ensure the vertical inheritance of plasmids by eliminating cells devoid of the plasmid post-segregation. Hence, we tested the capability of the two pairs in stabilizing exogenous pCA24N, a high-copy expression plasmid under relaxed copy number control that would generate plasmid-free cells in the K-12 host without selection pressure after continuous cultivation. As expected, both HicA^{T}B and StbDE effectively stabilized pCA24N plasmids for 480 generations without adding antibiotics, while half of the empty plasmids were lost after 240 generations (Supplementary Fig. S1C). However, this stabilization of a relaxed copy number plasmid by overexpressing a TA operon may not reflect adequately the physiological conditions in which TA systems stabilize conjugative plasmids with their lower and native expression levels.

Therefore, we next pursued more physiologically-relevant conditions to investigate plasmid stability and the physiological role of these two TA systems on the p45 plasmid. Since the wild-type (WT) p45 is maintained at approximately one copy per cell in the K-12 host, we constructed deletions to knock out each toxin gene and each TA pair from p45. In the absence of polymyxin B (PB), the p45 plasmid was stably maintained at approximately one copy per cell in K-12, indicating that the replication and segregation of p45 are under stringent control. In addition, the mutant plasmids p45Δ*stbE* or p45Δ*stbDE* did not affect the growth of the host cells and the plasmid conjugation frequency (Supplementary Fig. S2). Like deleting *stbE*, deleting *hicA* did not affect plasmid stability or replication, resulting in the isogenic plasmid p45Δ*hicA* with the same copy number as the WT p45. However, when the *hicAB* operon was targeted for deletion, the WT p45 plasmid still coexisted with the p45Δ*hicAB* plasmid within the cell in the presence of Cm, which was used to select for the targeted deletion of the *hicAB* operon. This observation suggests that complete removal of *hicAB* could not be achieved directly via the same approach (Fig. 2A). We denoted the deletion strain with two mixed plasmids as K-12/p45: p45Δ*hicAB*. Increasing the Cm concentration to select p45Δ*hicAB* during genetic manipulation or continuous culture of the K-12/p45: p45Δ*hicAB* strain with Cm was unable to eliminate the WT p45 plasmid. Two alternative approaches were then applied to obtain K-12/p45Δ*hicAB*: supplementing the HicB antitoxin from a different plasmid or knocking out the *hicB* gene from the K-12/p45Δ*hicA* host (Fig. 2B and Supplementary Fig. S3). The p45Δ*hicAB* plasmids were confirmed by sequencing, and no intentional mutations were found.

The p45 isogenic plasmid lacking the *hicA* or *stbE* toxin gene was stably maintained in host cells after 160 generations (20 generations/transfer) in the absence of antibiotics (Supplementary Fig. S4 and Fig. 3A). Quantitative PCR (qPCR) revealed that the plasmid copy number per cell did not change after the toxin gene was removed. Importantly, we found that plasmids lacking *stbDE* or *hicAB* TA loci were also stably maintained in host cells, with approximately one copy per cell in the absence of antibiotics (Fig. 2C and D, and Supplementary Fig. S4). To investigate whether the presence of either single TA system is sufficient to stabilize p45, we further knocked out *stbDE* from K-12/p45Δ*hicAB*, resulting in the K-12/p45Δ*hicAB*Δ*stbDE* strain lacking both TA systems (Fig. 2E). Unexpectedly, the p45Δ*hicAB*Δ*stbDE* plasmid was also stably maintained in the K-12 host at approximately one copy per cell (Fig. 2F–H). Importantly, cell viability and conjugative transfer were not affected by removing the toxin gene or the TA pairs (Supplementary Figs S2 and S4).

To exclude the possibility that plasmid conjugation contributes to the reintroduction of the p45 plasmid lacking *hicAB* and *stbDE* into plasmid-free cells that may have occurred postsegregation, we knocked out the origin of transfer (*oriT*) sites in both p45 and p45Δ*hicAB*Δ*stbDE*. The p45 plasmid carries the *nikAB* gene, which mediates the initiation of conjugative transfer, similar to the *oriT* region of the R64 plasmid [53]. On the basis of the sequence characteristics of the *oriT* region in the R64 plasmid, we identified and knocked out a potential *oriT* region in p45 (Supplementary Fig. S5). The results showed that knocking out *oriT* did not affect the copy number of p45 and confirmed that p45 was unable to undergo conjugative transfer (Fig. 2F). In the K-12/p45Δ*hicAB*Δ*stbDE* strain, the knockout of oriT blocked the effect of plasmid horizontal transfer on plasmid occupancy (Fig. 2F). The p45Δ*hicAB*Δ*stbDE*ΔoriT plasmid was stably maintained in the K-12 host at approximately one copy per cell (Fig. 2F and G). The results from green fluorescence microscopy showing that all cells carrying p45Δ*hicAB*Δ*stbDE*ΔoriT also supported this finding (Fig. 2H), indicating that *hicAB* and *stbDE* do not confer vertical stability to the p45 plasmid.

HicAB confers a competitive advantage over StbDE in terms of plasmid–plasmid competition

The greater occurrence of *hicAB* than *stbDE* in *mcr-1*-associated IncI2 plasmids (Fig. 1C) and the partial deletion of *hicAB*, as opposed to *stbDE* (Fig. 2A), suggest that HicAB and StbDE serve distinct functions within the plasmid. To further investigate the competition between the p45 and p45Δ*hicAB* plasmids coexisting in the same host, a qPCR assay was applied to monitor the dynamic changes in the two plasmids using primers to amplify the *hicAB* gene (*hicAB*-qF/qR) and the Cm resistance gene (*cm*-qF/qR). The copy number of the plasmid was also quantified using the chromosomal single-copy gene *gapdh* (*gapdh*-qF/qR) as a reference. Initially, single colonies of the K-12/p45: p45Δ*hicAB* strain growing on selective plates (LB + Cm) (depicted as G0) were cultured in LB with Cm until they reached the exponential phase (OD_{600} ~0.8) (depicted as G1). At the G0 stage, the WT and the mutant p45 plasmids were equally present in the host population, and the copy number was ~2 (Supplementary Fig. S6A). Successive generations were obtained by reinoculating 1/1000 of the previous culture into fresh LB. Moreover, serial dilutions from every 40 generations were spotted on LB, LB with Cm, and LB with PB plates (Fig. 3A), and qPCR was performed (Fig. 3B). The results revealed a decreasing frequency of the p45: p45Δ*hicAB* strain on the Cm plates with increasing generations, whereas the ratio of p45 to p45Δ*hicAB* plasmids increased significantly, reaching >1500:1 at G80 (Fig. 3B). Accordingly, the copy number of

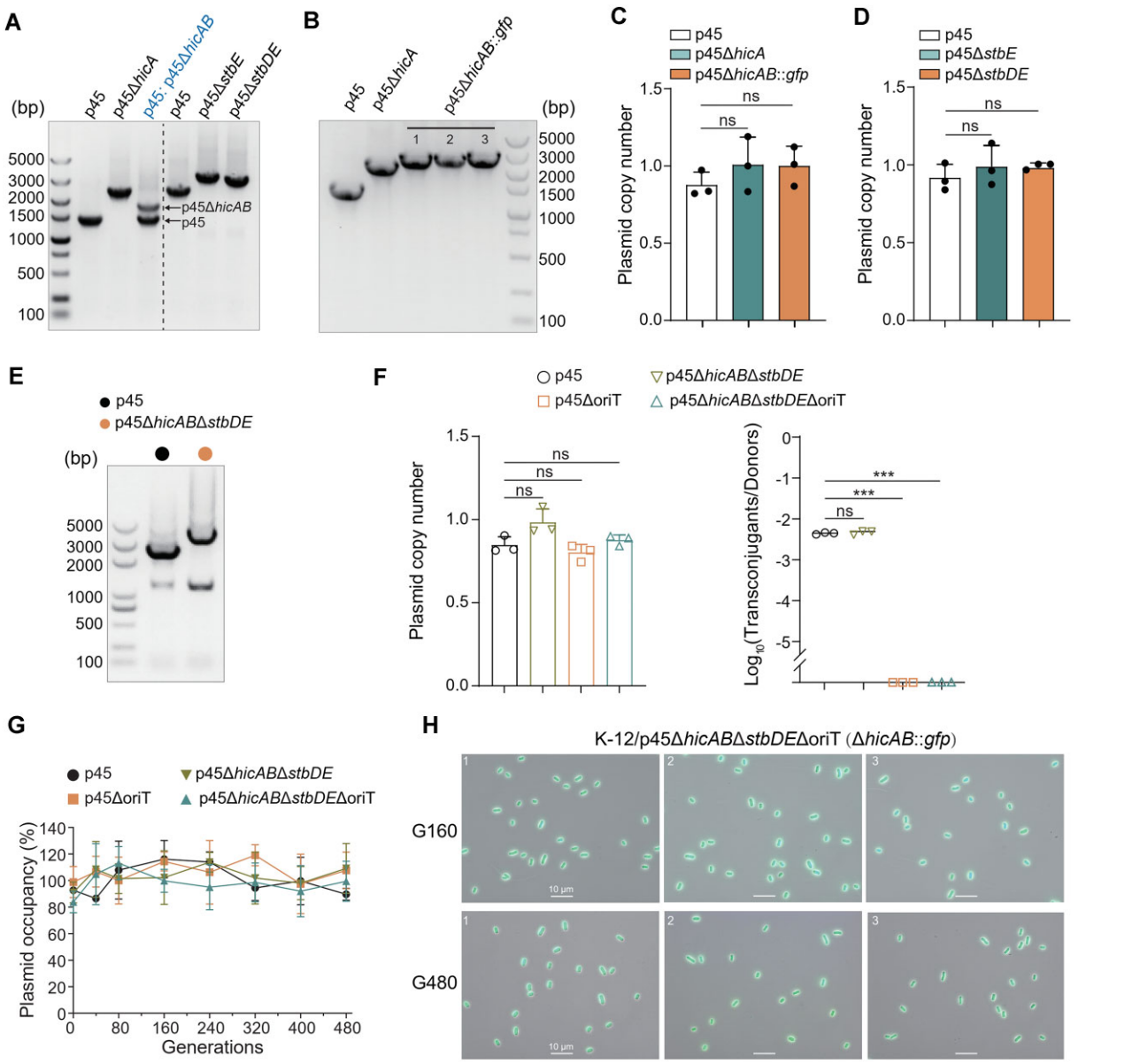

Figure 2. HicAB and StbDE are both dispensable for the vertical stability to the p45 plasmid. (**A**, **B**) The deletion of TA systems was confirmed via PCR, and the deleted TA genes were substituted with a Cm resistance gene or Kan resistance gene. (**C**, **D**) Copy numbers of p45, *hicA*, *hicAB*, *stbE*, and *stbDE* deletion mutants. (**E**) Double deletion of the TA system was confirmed via PCR. (**F**) Copy numbers and conjugation frequency of p45, p45Δ*hicAB*Δ*stbDE*, p45Δ*oriT*, and p45Δ*hicAB*Δ*stbDE*Δ*oriT* in the K-12 strain. (**G**) Plasmid stability determination of p45, p45Δ*hicAB*Δ*stbDE*, p45Δ*oriT*, and p45Δ*hicAB*Δ*stbDE*Δ*oriT* in the K-12 strain. (**H**) Microscopic observation of K-12/p45Δ*hicAB*Δ*stbDE*Δ*oriT* at G160 and G480 in LB. For panels (C), (D), (F), and (G), the quantified data from different experiments are presented as the mean ± standard deviation (SD) of three biological replicates. The *P*-values were calculated with two-tailed Student's *t*-tests (ns, not significant; ***$P < .001$). Representative images are shown in panel (H).

K-12/p45: p45Δ*hicAB* at G160 was ~1, as most cells carried p45 (Supplementary Fig. S6A). These results indicate that WT p45 has a strong competitive advantage over p45Δ*hicAB* during plasmid–plasmid competition when they are present in the same host cell.

In parallel, to explore the role of StbDE in plasmid–plasmid competition, we employed conjugative transfer to obtain the strain K-12/p45: p45Δ*stbDE* harboring the p45 plasmid and the p45Δ*stbDE* plasmid. The copy number of the p45: p45Δ*stbDE* in K-12 after conjugation is about 2 at G0 (Supplementary Fig. S6B). In the absence of antibiotics, p45 showed a much weaker advantage over p45Δ*stbDE* compared with p45 over p45Δ*hicAB*, since the ratio of p45 to p45Δ*stbDE* plasmids reached 17:1 at G80 (Fig. 3C). Furthermore, to explore which of HicAB and StbDE has a greater competitive advantage in plasmid–plasmid competition, we employed conjugative transfer to obtain the strain K-12/p45Δ*stbDE*: p45Δ*hicAB* harboring the p45Δ*stbDE* plasmid and the p45Δ*hicAB* plasmid. In the absence of antibiotics, p45Δ*stbDE* showed a competitive advantage over p45Δ*hicAB*, since the ratio of p45Δ*stbDE* to p45Δ*hicAB* plasmids reached 750:1 at G8 (Fig. 3D). Taken together, the above results confirmed that HicAB confers a competitive advantage over StbDE in terms of plasmid–plasmid competition.

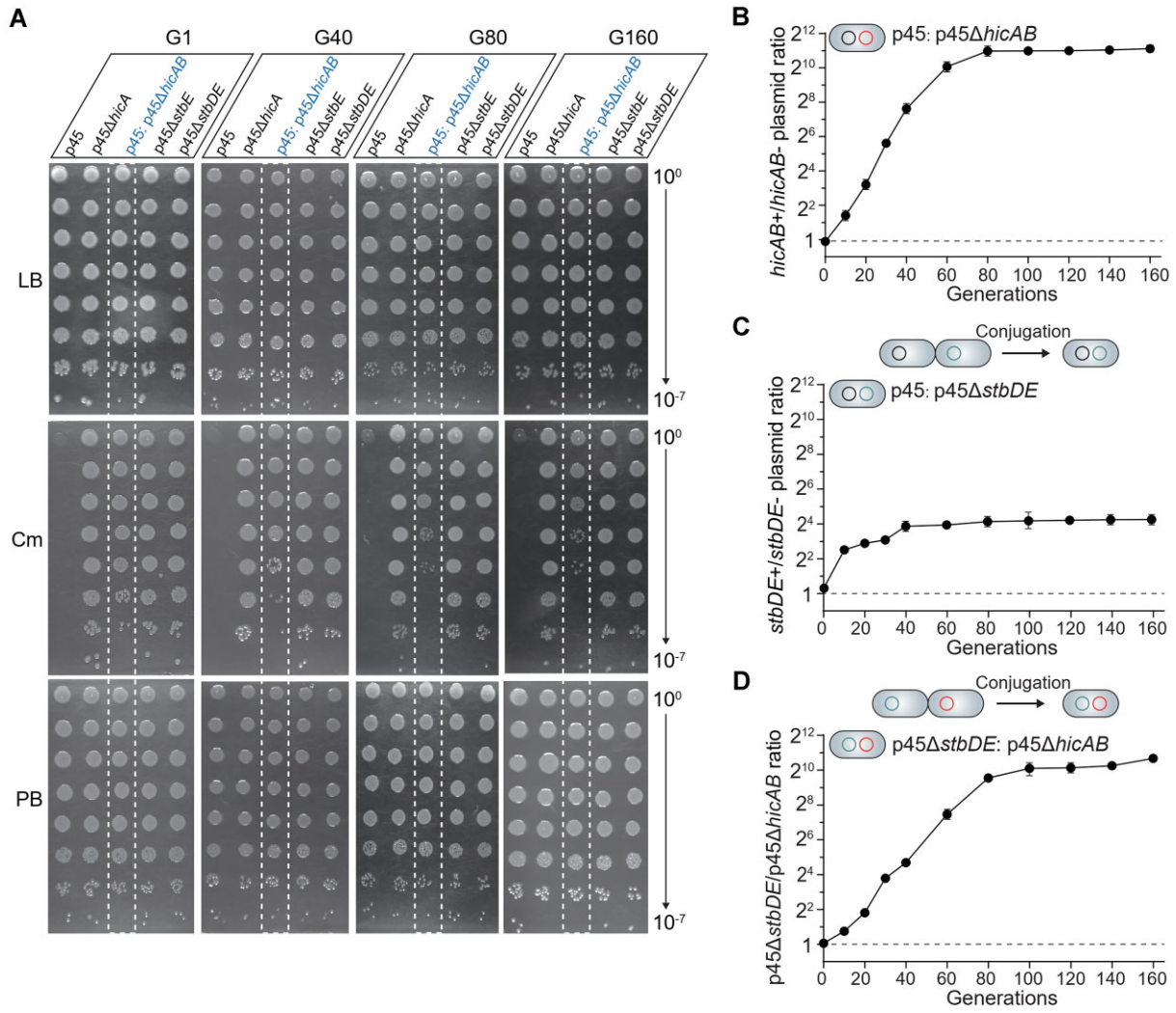

Figure 3. HicAB confers a competitive advantage over StbDE in terms of plasmid–plasmid competition. (**A**) Plasmid stability of p45 and TA mutants in K-12 [with ∼20 min/generation (G)]. The TA mutants cultivated in LB with Cm, denoted as G1 before being transferred to LB, were subcultured in LB at intervals of 20 G. (**B**) The ratio of plasmids (p45 versus p45Δ*hicAB*) was determined in the K-12/p45: p45Δ*hicAB* strain at serial generations. (**C**) The ratio of plasmid (p45 versus p45Δ*stbDE*) was determined in the K-12/p45: p45Δ*stbDE* strain at serial generations. (**D**) The ratio of plasmid (p45Δ*stbDE* versus p45Δ*hicAB*) was determined in the K-12/p45Δ*stbDE*: p45Δ*hicAB* strain at serial generations. For panels (B)–(D), the data are from three independent cultures, and SDs are shown. Representative images are shown in panel (A).

HicA^{T}B mediated plasmid–plasmid competition via a noncanonical intrinsic terminator

Next, we aimed to investigate why HicAB and StbDE differ in how they impact plasmid competition. For type II TAs, the TA operon is usually cotranscribed with the antitoxin gene preceding the toxin gene [6]. On the p45 plasmid, the *hicA* toxin-encoding gene lies upstream of *hicB*, and the open reading frames (ORFs) of the two genes are separated by 24 bp. For *stbDE*, the ORFs of the *stbD* antitoxin and *stbE* toxin overlap by 11 bp (Fig. 1D). Cotranscription assays revealed that the toxin and antitoxin genes of the two TA operons are cotranscribed (Fig. 1H). In addition, the primer extension experiments also indicated that *stbDE* was cotranscribed and that *hicAB* possesses distinct transcriptional start sites (Fig. 1I). However, RNA-seq of p45 revealed that the abundance of *hicA* messenger RNA (mRNA) was ∼10-fold greater than that of *hicB*, with a sharp decrease in RNA abundance after the *hicA* coding region, whereas the abundances of *stbD* and *stbE* mRNAs were both low and similar (Fig. 4A).

To further investigate the differential expression of *hicA* and *hicB*, we analyzed the transcription termination of the TA operon. The canonical intrinsic terminator forms a G/C-rich hairpin structure in the RNA, followed by a 7- to 8-nt U-rich tract in the RNA: DNA hybrid [54, 55]. Both the *hicAB* and *stbDE* operons have a canonical intrinsic terminator at the end of the TA transcripts, featuring a G/C-rich hairpin followed by a U-rich tract ($n = 8$) (Fig. 4B). Unexpectedly, we also found another intrinsic terminator-like G/C-rich hairpin in the *hicAB* intergenic region with a short U tract ($n = 3$) (Fig. 4C); we renamed this subfamily of HicAB containing the *hicA*-specific terminator HicA^{T}B.

To explore whether this internal terminator affects the mRNA abundance of *hicA* and *hicB*, targeted deletion was performed to construct the mutant plasmid p45ΔTer (Fig. 4C). In the presence of the *hicA*-specific terminator, similar to the RNA-seq results, the abundance of *hicA* mRNA was ∼10-fold greater than that of *hicB* (Fig. 4D and E). Conversely, in the absence of this terminator, the mRNA abundance of *hicA*

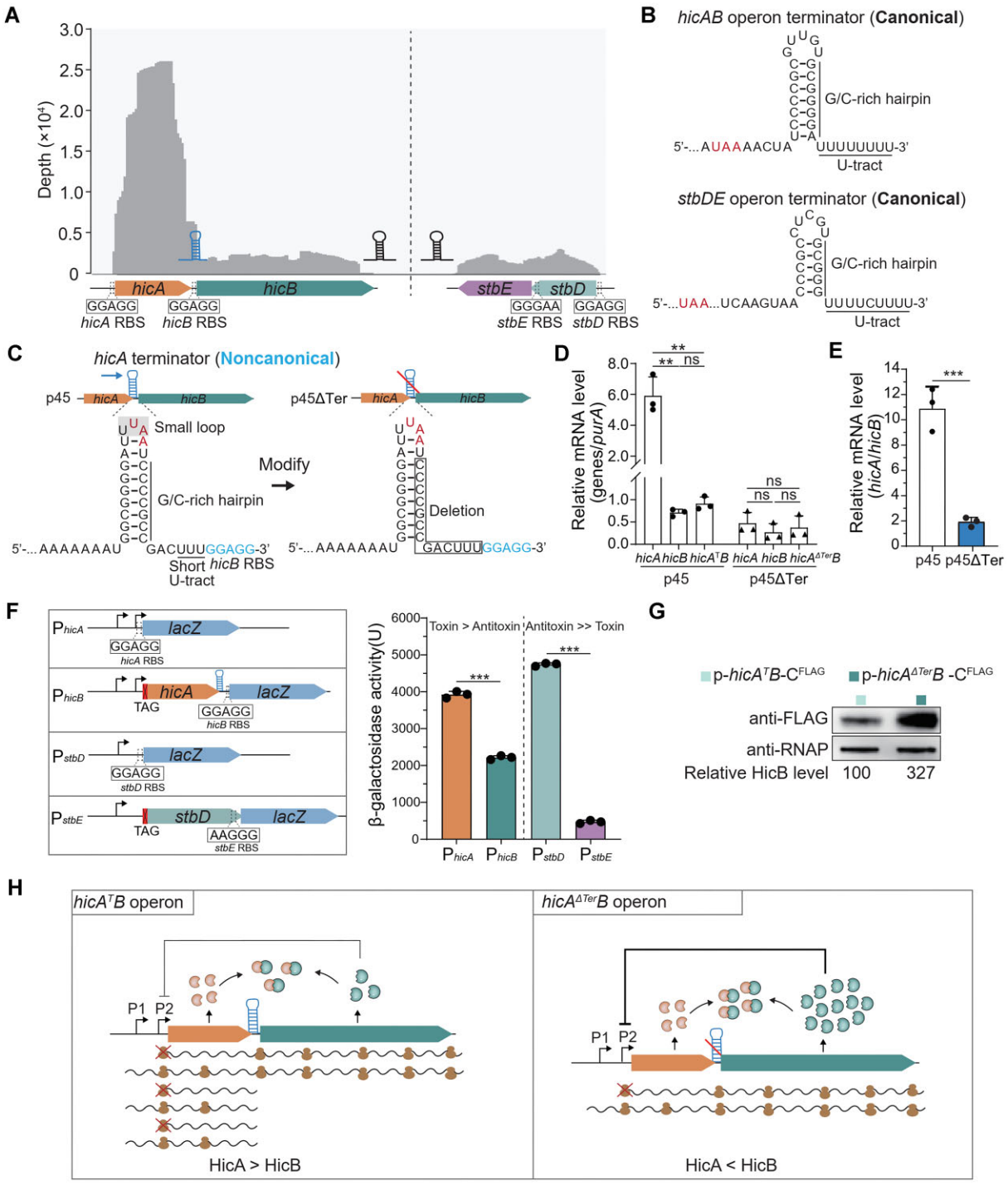

Figure 4. The noncanonical intrinsic terminator is essential for the imbalanced HicA:HicB ratio. (**A**) Depth of *hicA*, *hicB*, *stbD*, and *stbE* transcripts in the K-12/p45 strain. (**B**) Diagram of the intrinsic terminator for the *hicA*^{T}*B* and *stbDE* TA operons. (**C**) Diagram depicting the *hicA*-specific intrinsic terminator and the ΔTer mutant, where a 13-bp deletion disrupts the terminator structure. (**D**) The relative mRNA levels of *hicA*, *hicB,* and *hicA*^{T}*B* to the reference gene *purA* in the K-12/p45 and K-12/p45ΔTer strains. (**E**) The relative mRNA levels of *hicA* to *hicB* in the K-12/p45 and K-12/p45ΔTer strains. (**F**) The translation efficiencies of the indicated TA genes were measured using pHGR01-P$_{hicA}$-*lacZ*, pHGR01-P$_{hicB}$-*lacZ*, pHGR01-P$_{stbD}$-*lacZ*, and pHGR01-P$_{stbE}$-*lacZ*. (**G**) Western blot showing the production of HicB protein in the K-12/pBBR1Cm-*hicA*^{T}*B*-C^{FLAG} and K-12/pBBR1Cm-*hicA*$^{\Delta Ter}$*B*-C^{FLAG} strains using a FLAG-tag at the C-terminus of HicB (17.1 kDa). RNAP was used as a control. (**H**) Model for the role of the *hicA*-specific terminator in determining the toxin/antitoxin ratio. For panels (D)–(F), the quantified data from different experiments are presented as the mean ± SD of three biological replicates. The *P*-values were calculated with two-tailed Student's *t*-tests (ns, not significant; $^{**}P < .01$; $^{***}P < .001$). Representative images are shown in panels (A) and (G).

was similar to that of *hicB* (Fig. 4E). These results demonstrate that the presence of an internal terminator in the *hicA* toxin gene upstream of *hicB* specifically resulted in a reduced abundance of HicB antitoxin transcripts.

To further explore the production of TA at the protein level, we analyzed the ribosome binding site (RBS) of the TA operons. For HicA^{T}B, the toxin and antitoxin genes each have a strong RBS (5′-GGAGG), suggesting that the toxin protein should be produced more than the antitoxin protein, primarily on the basis of the different numbers of transcripts, not on the basis of differences in translation. In contrast, for StbDE, the antitoxin still has a strong RBS (5′-GGAGG), but the toxin has a relatively weaker RBS (5′-AAGGG), indicating that the antitoxin should be produced in excess of the toxin (Fig. 4A). Translational lacZ fusions for monitoring protein production were constructed, and we found that the two TA pairs do indeed differ in toxin and antitoxin production. For StbDE, 9-fold more antitoxin than toxin was produced. In contrast, for HicA^{T}B, the toxin was produced at a significantly greater level than the antitoxin was (Fig. 4F, right panel). These results were consistent with the toxicity test results, which revealed that *hicA^{T}B* was less viable than stbDE when the pBAD-based vector was used, as the toxin was produced in excess of the antitoxin for the *hicA^{T}B* TA pair but was the opposite for the *stbDE* TA pair (Fig. 1D). Furthermore, the *hicA*-specific terminator with a long G/C-rich hairpin lies precisely upstream of the RBS of *hicB*. Western blotting with Flag-tagged HicB revealed that the presence of the G/C-rich hairpin reduced HicB translation (Fig. 4G). Toxicity test assays with a high-copy pUC19 plasmid carrying the *hicA^{T}B* operon and its native promoter also showed significant toxicity in K-12, which was reduced by deleting the internal terminator within the operon (Supplementary Fig. S7A). Upon deleting the *hicA*-specific terminator, the HicB protein level increased, intensifying its self-repression on the P2 promoter and consequently leading to a reduction in the mRNA levels of *hicA^{T}B* [56] (Fig. 4D and Supplementary Fig. S7B and C). In conclusion, although StbDE and HicA^{T}B are both type II TA pairs, they differ in toxin production. Importantly, the presence of a *hicA*-specific terminator inside the *hicAB* operon contributes to a higher toxin: antitoxin ratio (Fig. 4H). In *E. coli* K-12 MG1655, *hicAB* is transcribed from two promoters [56]. The P2 promoter, with a short 5′ untranslated leader just 1 base upstream of the RBS of *hicA* translates *hicB* but not *hicA* [56], which is consistent with our study of *hicAB* (Fig. 4H). In addition, unlike type II antitoxin MqsA [57], the HicB antitoxin remained stable in the presence of K-12 lysates for up to 12 h (Supplementary Fig. S7D–G), suggesting that HicA activation is less likely via HicB degradation.

A recent study reported that an HicAB TA encoded by the IncX4 plasmid pJIE143 could be directly deleted using the same one-step method [28], suggesting that this *hicAB* may function differently from the HicA^{T}B TA studied here. Our analysis revealed that HicAB does not have an intrinsic terminator and that the ORFs of the two TA genes overlap; thus, we named it the HicA^{O}B TA pair. Next, 825 pairs of *hicABs* located on the IncI2 and IncX4 plasmids were reanalyzed, and we found that they could be classified into two subfamilies. Intriguingly, *hicA^{T}B* is predominant on IncI2 plasmids, and *hicA^{O}B* is predominant on IncX4 plasmids (Fig. 5A). The *hicA^{T}B* subfamily featured an internal intrinsic terminator highly conserved in the intergenic region, highly similar to the *hicA^{T}B* system found on p45 (Fig. 5B). Conversely, the *hicA^{O}B* subfamily has no internal intrinsic terminator, and the ORFs of the TA genes overlap, which is highly similar to the *hicA^{O}B* on pJIE143 (Fig. 5B). The HicA and HicB genes between the two subfamilies had intermediate levels at the nucleotide level (~47.5%) (Fig. 5B) and low sequence identity at the protein level (<26%) (Fig. 5C), suggesting that they may have evolved differently. Cell viability assays conducted in K-12 cells demonstrated that HicA from the p14EC007a plasmid acts as a toxin, whereas HicB serves as its corresponding antitoxin, completely neutralizing the toxicity of HicA (Fig. 5D). We then determined whether the intrinsic terminator inside the TA operon contributes to the difference in TA function. For the two *hicAB* operons, the *hicA* mRNA level in *hicA^{T}B* was much higher (~10-fold) than that in the chromosome reference gene *purA*, whereas the *hicA* mRNA level in *hicA^{O}B* was not (Fig. 5E). The level of *hicA* mRNA was significantly greater than that of the cognate *hicB* in the *hicA^{T}B* TA operons. As expected, similar to deleting the terminator in *hicA^{T}B*, the *hicA* and *hicB* mRNAs in *hicA^{O}B* were similar (Fig. 5F). In further investigations, we obtained *E. coli* C600/p14EC007a: p14EC007aΔ*hicA^{O}B* via conjugation and then evaluated the competition between these two plasmids within the host *E. coli* C600. In the absence of antibiotics, the p14EC007a IncX4 plasmid showed a limited advantage over p14EC007Δ*hicA^{O}B*, since the ratio of the p14EC007a plasmid to the p14EC007Δ*hicA^{O}B* plasmid reached 3:1 at G80 (Fig. 5G).

Building upon the preceding findings, we hypothesized that HicA^{T}B relies on the native production of HicA to mediate plasmid–plasmid competition. To experimentally validate this, we conducted plasmid competition using modified isogenic plasmids either lacking the *hicA* gene (p45Δ*hicA*) or deleting the *hicA*-specific terminator (p45ΔTer) to compete with p45Δ*hicA^{T}B*. As expected, p45 was maintained far more than p45Δ*hicA^{T}B*, whereas there were no differences for p45Δ*hicA* versus p45Δ*hicA^{T}B* and p45ΔTer versus p45Δ*hicA^{T}B*, indicating that the internal *hicA*-specific terminator resulting in a high ratio of HicA to HicB is indispensable for gaining advantages during plasmid competition (Fig. 6A-C).

The parental K-12/p45: p45Δ*hicA^{T}B* cells should generate daughter cells carrying p45, p45: p45Δ*hicA^{T}B*, and p45Δ*hicA^{T}B*. Time-lapse microscopic observations were performed to monitor PSK during the division of K-12/p45: p45Δ*hicA^{T}B*. Without the maintenance of the Cm antibiotic, some elongated cells presented delayed cell division (marked with yellow circles) (Fig. 6D and Supplementary Movie S3). In contrast, the division of K-12 cells harboring p45 (Supplementary Movie S1) or p45Δ*hicA* (Supplementary Movie S2) was normal. Therefore, increased HicA production in K-12 cells led to the formation of aberrant and elongated cells (Fig. 6E). The growth assay further showed that overexpression of HicA in the host cell lacking a *hicB* gene appeared more toxic compared to overexpression of HicA in the presence of *hicB* (Supplementary Fig. S8). We thus reasoned that the cells incapable of dividing were those carrying p45Δ*hicA^{T}B*, and cell division and plasmid competition between p45: p45Δ*hicA^{T}B* with and without the addition of Cm were depicted at generations G0 and G1 and post-competition at G160 (Fig. 6F). Overall, we demonstrated that HicA^{T}B mediated plasmid competition via toxin production and that the presence of the intrinsic terminator inside the TA operon is indispensable for this function.

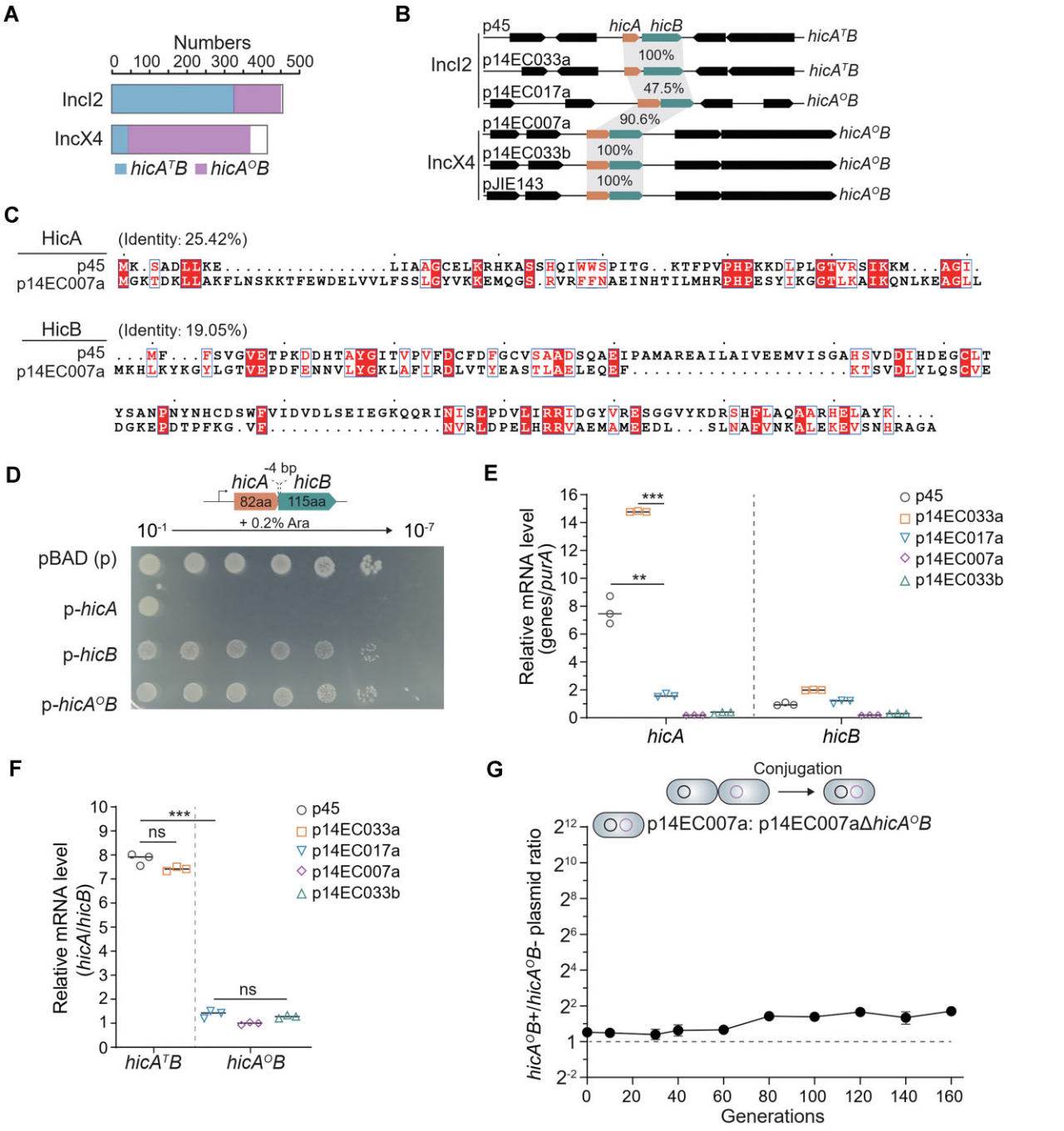

Figure 5. The p14EC007a plasmid showed a very slight advantage over p14EC007Δ*hicA*^{O}*B*. (**A**) Distribution of the two subfamilies of *hicAB* in the IncI2 and IncX4 plasmids. (**B**) Selected IncI2 and IncX4 plasmids harboring two subfamilies of the *hicAB* TA system were compared at the nucleotide sequence level. (**C**) Protein alignment of HicA and HicB in two subfamilies of *hicAB* from the p45 and p14EC007a plasmids. (**D**) Toxicity test of TA system from the p14EC007a plasmid in K-12 via pBAD (p) under the induction of 0.2% *L*-arabinose. (**E**) mRNA levels of *hicA* and *hicB* to the reference gene *purA* in selected IncI2 and IncX4 plasmids. (**F**) The relative mRNA levels of *hicA* to *hicB* in selected IncI2 and IncX4 plasmids. (**G**) The ratio of plasmid (p14EC007a::*cm* versus p14EC007aΔ*hicA*^{O}*B*) was determined in the *E. coli* C600/p14EC007a: 14EC007aΔ*hicA*^{O}*B* strain at serial generations. For panels (E)–(G), the quantified data are presented as the mean ± SD of three biological replicates. The *P*-values were calculated with two-tailed Student's *t*-tests (ns, not significant; $^{**}P < .01$; $^{***}P < .001$). The data are from three independent cultures, and SDs are shown. A representative image is shown in panel (D).

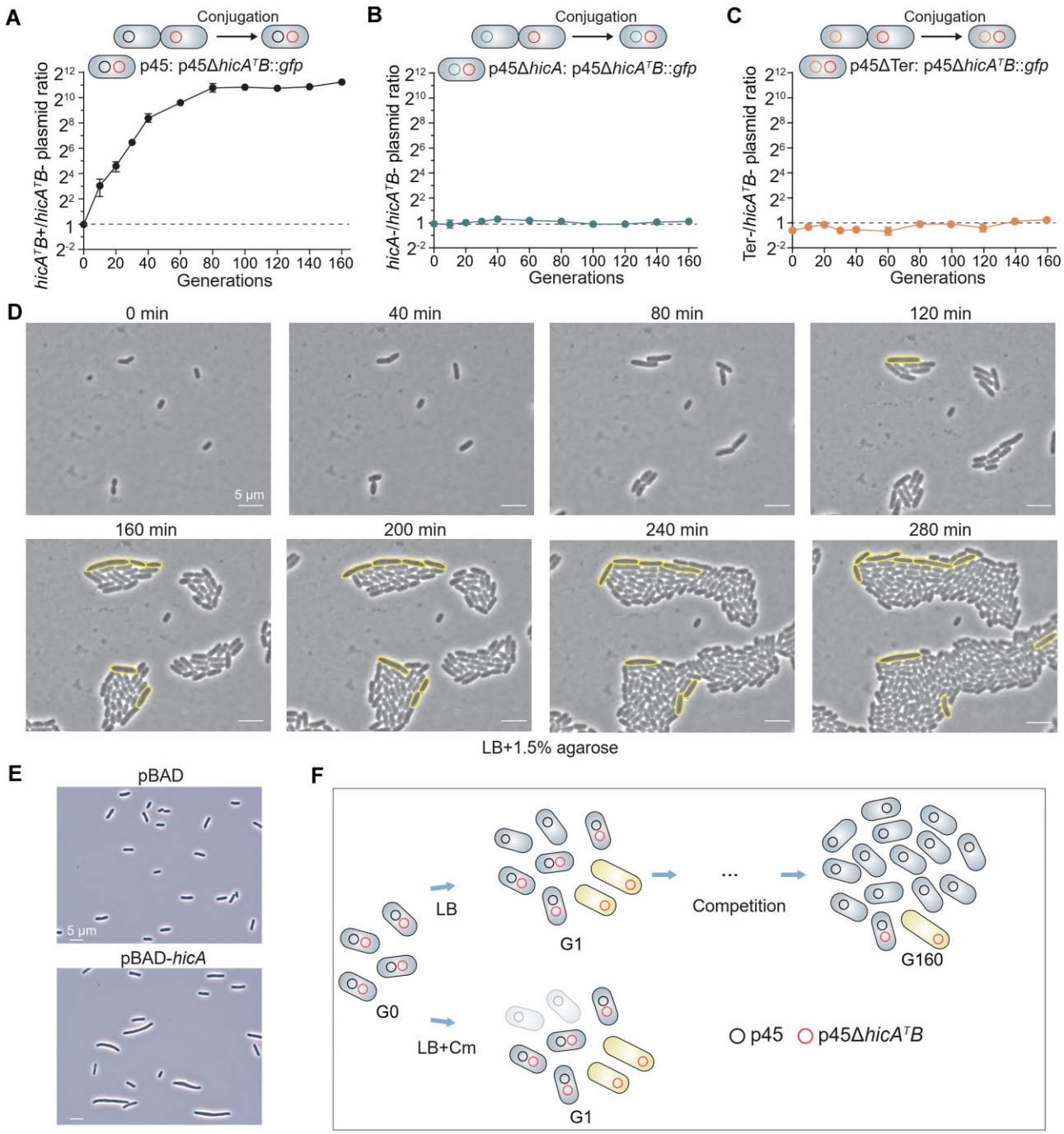

Figure 6. HicA^{T}B mediated plasmid competition via a noncanonical intrinsic terminator. (**A**) The ratio of plasmids (p45 versus p45Δ*hicA*^{T}*B*) was determined in the K-12/p45: p45Δ*hicA*^{T}*B::gfp* strain at serial generations. (**B**) The ratio of plasmids (p45Δ*hicA* versus p45Δ*hicA*^{T}*B*) was determined in the K-12/p45Δ*hicA*: p45Δ*hicA*^{T}*B::gfp* strain at serial generations. (**C**) The ratio of plasmid (p45ΔTer versus p45Δ*hicA*^{T}*B*) was determined in the K-12/p45ΔTer: p45Δ*hicA*^{T}*B::gfp* strain at serial generations. (**D**) Time-lapse observations under the microscope were conducted at serial time points for the K-12/p45: p45Δ*hicA*^{T}*B* strain. The elongated cells with delayed division are outlined. (**E**) HicA was produced via pBAD-*hicA* using 0.3% *L*-arabinose as an inducer in *E. coli* ER2738. (**F**) Diagram depicting the plasmid–plasmid competition of host cells containing one copy of p45 and one copy of p45Δ*hicA*^{T}*B* prior to competition (G0, G1) and post-competition at G160. For panel (A)–(C), the data are from three independent cultures, and SDs are shown. Representative images are shown in panels (D) and (E).

HicA^{T}B and StbDE in p45 promote plasmid transmission in host cells

To further investigate the role of TA systems in mediating host–plasmid competition, we determined host phenotypic alterations, including swimming motility, antibiotic resistance, biofilm formation, and phage defense, after deleting each TA system (Supplementary Fig. S9A–D). A reduction in swimming motility and slower cell growth in biofilm formation were observed following the conjugation of the p45 plasmid into the K-12 host, suggesting a potential fitness cost associated with the p45 plasmid. However, neither the HicA^{T}B nor the StbDE TA systems seem to have a significant effect on the K-12 host (Supplementary Fig. S9A–D).

Next, according to the above study, the two TA systems are expected to contribute to p45 fitness during bacterial competition via plasmid conjugation and/or plasmid competition within the host. We mixed the plasmid-free K-12 strain, with K-12 carrying one copy of K-12/p45, p45Δ*hicA^{T}B*, or p45Δ*stbDE* at an initial ratio of 4:1:1:1. These mixed populations were subsequently subjected to competition in the absence of antibiotics (Fig. 7A). The results showed that the K-12 bearing plasmids quickly became predominant over the plasmid-free K-12 cells after 1 day (Fig. 7B). As expected, cells harboring p45 plasmids have a competitive advantage than those cells harboring plasmids lacking *hicA^{T}B* or *stbDE* TA system (Fig. 7C). At the end of 7 days, the ratio of p45: p45Δ*stbDE*: p45Δ*hicA^{T}B* was ∼4:3:2. We showed that knocking out *stbDE* or *hicA^{T}B* did not affect the conjugative ability (Supplementary Figs S2B and S4D), and deleting each TA had no significant impact on host fitness or vertical stability of the p45 plasmid; thus, the p45 most likely gained an advantage over p45Δ*hicA^{T}B* during plasmid conjugation and plasmid–plasmid competition. The ratio of p45 to p45Δ*hicA^{T}B* was ∼2:1 on day 7 when one plasmid was initially contained in one cell, whereas the ratio was ∼1500:1 at G80 within-host competition when two different plasmids were initially contained in one cell (Fig. 3B). These differences are most likely due to a low transfer frequency from the p45 plasmid to the K-12 host carrying a copy of p45Δ*hicA^{T}B* (Supplementary Fig. S10).

Horizontal transfer is a critical process for conjugative plasmids; TA-mediated plasmid competition can thus function in the exclusion of competing plasmids via toxin-based toxicity. In addition, from the perspective of TA modules, this plasmid competition also functions to promote the spread of a specific family of TA modules within the population. In the case of p45 plasmids, *hicA^{T}B* functions to exclude plasmids lacking this TA, and this process also makes *hicA^{T}B* a predominant TA pair, revealing that the selfish nature of the TA module ultimately contributes to horizontal plasmid transfer.

Discussion

In this study, we investigated the functions of two TA systems individually encoded by *mcr-1*-bearing conjugative plasmids and found that the HicA^{T}B TA pair plays a critical role in promoting plasmid horizontal transmission. Following the ban of colistin as a feed additive, the detection rate of IncX4 plasmids declined significantly faster than that of IncI2 plasmids [23]. Our results agreed well with the results of the *mcr-1*-bearing plasmid survey, which revealed that IncI2 plasmids carrying the HicA^{T}B pair were more persistent than lncX4 plasmids carrying the HicA^{O}B pair. However, using the native stringent control plasmid p45, we found that isogenic plasmids lacking StbDE, HicA^{T}B, or both TA pairs did not suffer from apparent plasmid loss with or without the ability to conjugate. Instead, by deleting each TA system from the native plasmid, we discovered that the p45 plasmid carrying the HicA^{T}B pair competed over isogenic plasmids lacking *hicA^{T}B*, whereas *stbDE* and *hicA^{O}B* TA had limited contributions to mediating horizontal transmission. These results, in accordance with the results of the prevalence assay, revealed a high occurrence of *hicA^{T}B* over *stbDE* on these plasmids. Furthermore, while both HicA^{T}B and HicA^{O}B are predicted to belong to the HicAB TA family, they exhibit distinct distributions across IncI2 and IncX4 *mcr-1*-associated plasmids. Compared with *hicA^{O}B*, *hicA^{T}B* provides a stronger competitive advantage for plasmids, further demonstrating that the function of TA systems may not be solely based on predictions from those from the same family. Interestingly, previous studies of different conjugative plasmids encoding *parDE* TAs, in which the toxin ParE belongs to the same family as the *stbE* toxin in p45, demonstrated that these plasmids can outcompete those lacking *parDE* within the same incompatibility group [30, 58, 59]. Recently, on the large conjugative plasmid pMBL6842 of marine bacteria, we discovered the type II TA pair PrpT/PrpA, in which the toxin also belongs to the ParE family and directly regulates plasmid replication via the binding of the antitoxin to the iterons in the plasmid replication origin [27]. This study not only emphasizes the importance of investigating plasmid-encoded TA systems within their native context but also highlights the diverse functions of type II TA systems encoded by different plasmid types.

Previous work has demonstrated that toxin production is tightly controlled by antitoxins under normal growth conditions at the transcriptional and translational levels [12]. As exemplified by the canonical type II TA pair StbDE in p45, the antitoxin gene precedes the toxin gene, and the two genes are cotranscribed and share a strong Rho-independent transcriptional terminator. At the translational level, the antitoxin has a strong RBS, whereas the toxin has a weaker RBS. These features ensure the controlled production of StbE toxin only under specific conditions when StbD is degraded. The *hicAB* genes were first reported to be inserted into the major pilus gene cluster in several strains of *Haemophilus influenzae* [60] and were predicted to constitute a family of TA systems in 2006 [61]. In the majority of *hicAB* operons, the *hicA* gene toxin often precedes the *hicB* gene [61, 62]. Notably, unlike previously studied type II antitoxins with unstructured N- or C-termini that are unstable, HicB appeared stable. Indeed, recent studies also showed that proteases like Lon preferentially degrade unstructured proteins but not structured antitoxins or the antitoxin bound to a toxin to form a tightly TA complex [11, 63, 64]. Therefore, the liberation of p45-encoded HicA is less likely through the degradation of HicB. Instead, we discovered that the conjugative plasmid-encoded HicA^{T}B TA operon adopted a different strategy to increase toxin expression. Although the two genes are cotranscribed, an internal intrinsic terminator causes premature termination immediately after the *hicA* toxin gene, resulting in higher levels of the toxin relative to the antitoxin. This increased toxin production is crucial for the transmission and persistence of lncI2 *mcr-1*-bearing plasmids. This study revealed the versatile way employed by different type II TA systems to allow the toxic function to be liberated. In addition to traditional antitoxin

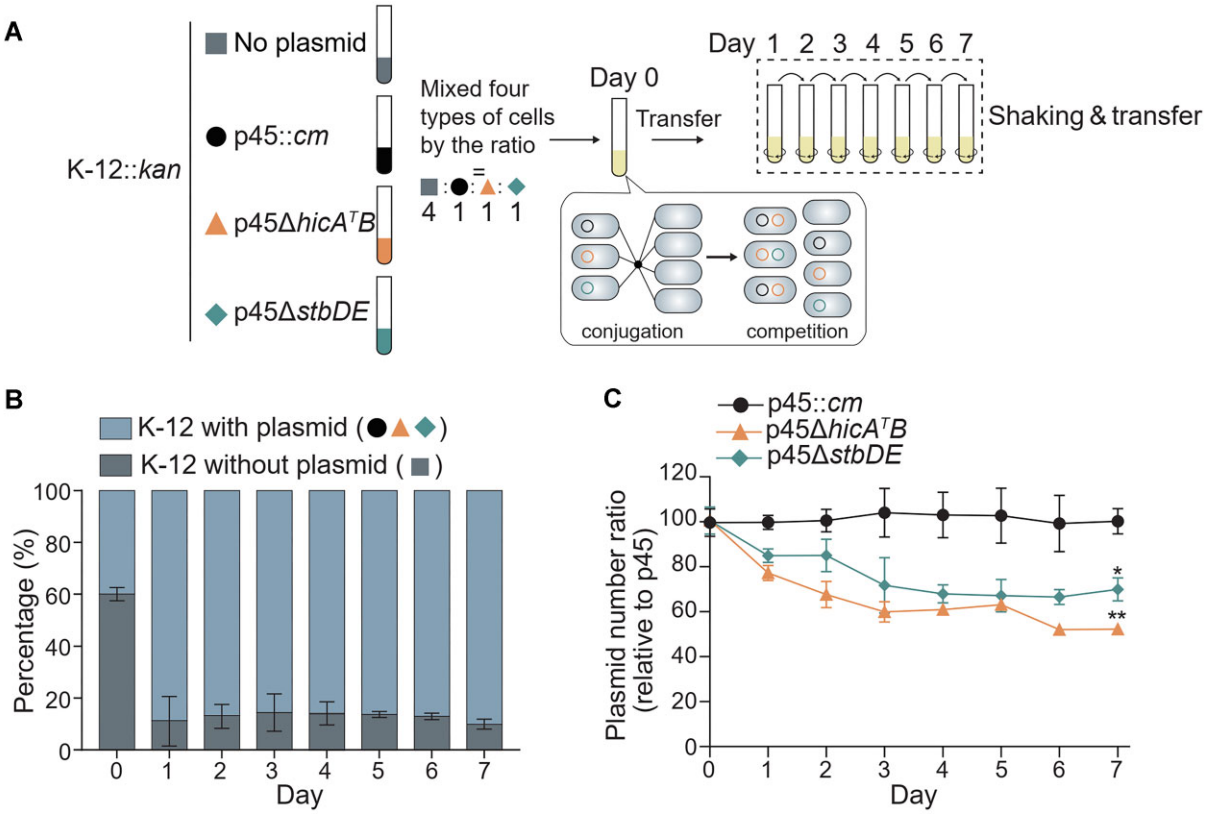

Figure 7. Bacteria carrying the p45 plasmid emerge as victors during bacterial competition. (**A**) Schematic diagram of the competition assay using the four different types of cells. (**B**) Percentages of K-12 harboring plasmids and plasmid-free K-12 during competition. The data are from three independent cultures, and SDs are shown. (**C**) Plasmid number ratios of p45::*cm*, p45Δ*hicA*^{T}*B*, and p45Δ*stbDE* during competition. The quantified data from different experiments are presented as the mean ± SD of three biological replicates. The *P*-values were calculated with two-tailed Student's *t*-tests for day 7 (*$P < .05$; **$P < .01$).

binding to regulate toxin release and activation, the regulation of TA expression at the transcription level could also be crucial for the execution of toxic function.

Additionally, HicAB TA systems display significant diversity, including the fusion of extra domains to either the HicA or HicB proteins [65]. Recent research has increasingly focused on the role of TA systems in antiphage defense [16]. Although the removal of *hicA*^{T}*B* or *stbDE* from p45 did not impact host resistance to various *E. coli* lytic phages, the role of phage-encoded HicAB systems in phage defense warrants further investigation.

The dissemination of ARGs such as *mcr-1* via conjugative plasmids involves horizontal transmission across different host cells and vertical inheritance during host cell propagation. The persistence of *mcr-1*-bearing conjugative plasmids post-ban as a feed additive is a good example of the 'plasmid paradox' [66, 67]. Despite the fitness cost conferred by the *mcr-1* gene and *hicA*^{T}*B* TA on host cells carrying these plasmids, the retention of these plasmids in the microbial community may reflect the 'selfish' nature of these mobile genetic elements. The integration of multiple ARGs, including *mcr-1*, into conjugative plasmids can be facilitated by transposons [68, 69]. Bacterial host cells acquire conjugative plasmids carrying ARGs in environmental niches where antibiotic resistance is crucial for survival, but they often prefer plasmids with a low copy number and high stability (e.g. IncI2 and IncX4) due to fitness costs [22, 70]. Our study demonstrated that IncI2 plasmids carrying the *hicA*^{T}*B* TA system with the incorporation of *mcr-1* confer a competitive advantage over plasmids lacking this TA pair. Notably, the *hicA*^{T}*B* TA loci on these plasmids induce addiction in the host through increased toxin production, ensuring persistence even when colistin resistance is no longer necessary. Our results align with the observed high co-occurrence of *mcr-1* and *hicA*^{T}*B* in IncI2 plasmids and the persistence of IncI2 plasmids in farmed animals, humans, food, and the environment even after colistin was banned as a feed additive in China [42]. Therefore, while reducing antibiotic use can mitigate the spread of specific ARGs, conjugative plasmids carrying TA systems remain significant vehicles for mediating the transfer of other ARGs facilitated by transposons, especially in environments such as the gut microbiome, where interspecies conjugation and competition for nutrients occur [71]. Our findings underscore the underestimated role of TA systems encoded by conjugative plasmids in driving ARG dissemination, suggesting that targeting these systems could help reduce the prevalence of conjugative plasmids in reservoirs and combat antibiotic resistance in the long term.

Acknowledgements

Author contributions: X.W.: Conceptualization, Project administration, Writing - review & editing; J.L., S.N., B.L., Y.G.: Methodology, Data curation, Investigation, Formal analysis, Writing- Original draft preparation; X.G., Y.L., L.Y., P.W.,

R.C., Y.J.: Software, Validation; T.W.: Writing - review & editing.

Supplementary data

Supplementary data is available at NAR online.

Conflict of interest

None declared.

Funding

This work was supported by the National Science Foundation of China (42188102, 31970037, 92451302, 32470032, 31625001, 32100030, 32100151), Science & Technology Fundamental Resources Investigation Program (2022FY100600), the Science and Technology Innovation Program of Hunan Province (2022RC1169), Local Innovative and Research Teams Project of Guangdong Pearl River Talents Program (2019BT02Y262), the special fund of South China Sea Institute of Oceanology, Chinese Academy of Sciences (SCSIO2023QY03), the Ocean Negative Carbon Emissions Program.

Data availability

The data supporting the findings of this study are available within the manuscript and its associated Supplementary Information. The RNA-seq of K-12/p45 and the next-generation sequencing of K-12/p45Δ*hicAB*::*gfp* raw data have been deposited in the Sequence Read Archive (SRA) under the BioProject accession number PRJNA1068435 and there are no restrictions on data availability. Additionally, the RNA-seq data of K-12/p45 has been deposited in the Gene Expression Omnibus (GEO) database under accession number GSE284789, with no data availability restrictions.

References

1. Ogura T, Hiraga S. Mini-F plasmid genes that couple host cell division to plasmid proliferation. *Proc Natl Acad Sci USA* 1983;**80**:4784–8. https://doi.org/10.1073/pnas.80.15.4784
2. Jaffe A, Ogura T, Hiraga S. Effects of the *ccd* function of the F plasmid on bacterial growth. *J Bacteriol* 1985;**163**:841–9. https://doi.org/10.1128/jb.163.3.841-849.1985
3. Bravo A, de Torrontegui G, Diaz R. Identification of components of a new stability system of plasmid R1, ParD, that is close to the origin of replication of this plasmid. *Mol Gen Genet* 1987;**210**:101–10. https://doi.org/10.1007/BF00337764
4. Gerdes K, Poulsen LK, Thisted T *et al.* The *hok* killer gene family in gram-negative bacteria. *New Biol* 1990;**2**:946–56.
5. Gerdes K, Christensen SK, Lobner-Olesen A. Prokaryotic toxin–antitoxin stress response loci. *Nat Rev Micro* 2005;**3**:371–82. https://doi.org/10.1038/nrmicro1147
6. Lin J, Guo Y, Yao J *et al.* Applications of toxin–antitoxin systems in synthetic biology. *Eng Microbiol* 2023;**3**:100069. https://doi.org/10.1016/j.engmic.2023.100069
7. Wang X, Wood TK. Cryptic prophages as targets for drug development. *Drug Resist Updat* 2016;**27**:30–8. https://doi.org/10.1016/j.drup.2016.06.001
8. Hayes F. Toxins-antitoxins: plasmid maintenance, programmed cell death, and cell cycle arrest. *Science* 2003;**301**:1496–9. https://doi.org/10.1126/science.1088157
9. Yao J, Guo Y, Wang P *et al.* Type II toxin/antitoxin system $ParE_{SO}$ /$CopA_{SO}$ stabilizes prophage CP4So in *Shewanellaoneidensis*. *Environ Microbiol* 2018;**20**:1224–39. https://doi.org/10.1111/1462-2920.14068
10. Wang X, Wood TK. Toxin-antitoxin systems influence biofilm and persister cell formation and the general stress response. *Appl Environ Microb* 2011;**77**:5577–83. https://doi.org/10.1128/AEM.05068-11
11. Jurenas D, Fraikin N, Goormaghtigh F *et al.* Biology and evolution of bacterial toxin–antitoxin systems. *Nat Rev Micro* 2022;**20**:335–50. https://doi.org/10.1038/s41579-021-00661-1
12. Pizzolato-Cezar LR, Spira B, Machini MT. Bacterial toxin–antitoxin systems: novel insights on toxin activation across populations and experimental shortcomings. *Curr Res Microb Sci* 2023;**5**:100204.
13. Yao J, Zhen X, Tang K *et al.* Novel polyadenylylation-dependent neutralization mechanism of the HEPN/MNT toxin/antitoxin system. *Nucleic Acids Res* 2020;**48**:11054–67. https://doi.org/10.1093/nar/gkaa855
14. Ren D, Bedzyk LA, Thomas SM *et al.* Gene expression in *Escherichia coli* biofilms. *Appl Microbiol Biotechnol* 2004;**64**:515–24. https://doi.org/10.1007/s00253-003-1517-y
15. Guo Y, Tang K, Sit B *et al.* Control of lysogeny and antiphage defense by a prophage-encoded kinase-phosphatase module. *Nat Commun* 2024;**15**:7244. https://doi.org/10.1038/s41467-024-51617-x
16. LeRoux M, Laub MT. Toxin-antitoxin systems as phage defense elements. *Annu Rev Microbiol* 2022;**76**:21–43. https://doi.org/10.1146/annurev-micro-020722-013730
17. Van Melderen L, Bernard P, Couturier M. Lon-dependent proteolysis of CcdA is the key control for activation of CcdB in plasmid-free segregant bacteria. *Mol Microbiol* 1994;**11**:1151–7. https://doi.org/10.1111/j.1365-2958.1994.tb00391.x
18. Lehnherr H, Yarmolinsky MB. Addiction protein phd of plasmid prophage P1 is a substrate of the ClpXP serine protease of *Escherichia coli*. *Proc Natl Acad Sci USA* 1995;**92**:3274–7. https://doi.org/10.1073/pnas.92.8.3274
19. Diago-Navarro E, Hernandez-Arriaga AM, Kubik S *et al.* Cleavage of the antitoxin of the *parD* toxin–antitoxin system is determined by the ClpAP protease and is modulated by the relative ratio of the toxin and the antitoxin. *Plasmid* 2013;**70**:78–85. https://doi.org/10.1016/j.plasmid.2013.01.010
20. LeRoux M, Culviner PH, Liu YJ *et al.* Stress can induce transcription of toxin–antitoxin systems without activating toxin. *Mol Cell* 2020;**79**:280–92. https://doi.org/10.1016/j.molcel.2020.05.028
21. Xue H, Cordero OX, Camas FM *et al.* Eco-evolutionary dynamics of episomes among ecologically cohesive bacterial populations. *mBio* 2015;**6**:e00552-15. https://doi.org/10.1128/mBio.00552-15
22. Yang J, Wang HH, Lu Y *et al.* A ProQ/FinO family protein involved in plasmid copy number control favours fitness of bacteria carrying *mcr-1*-bearing IncI2 plasmids. *Nucleic Acids Res* 2021;**49**:3981–96. https://doi.org/10.1093/nar/gkab149
23. Liu YY, Zhou Q, He W *et al.* *mcr-1* and plasmid prevalence in *Escherichia coli* from livestock. *Lancet Infect Dis* 2020;**20**:1126. https://doi.org/10.1016/S1473-3099(20)30697-6
24. Gerdes K, Rasmussen PB, Molin S. Unique type of plasmid maintenance function: postsegregational killing of plasmid-free cells. *Proc Natl Acad Sci USA* 1986;**83**:3116–20. https://doi.org/10.1073/pnas.83.10.3116
25. Million-Weaver S, Camps M. Mechanisms of plasmid segregation: have multicopy plasmids been overlooked? *Plasmid* 2014;**75**:27–36. https://doi.org/10.1016/j.plasmid.2014.07.002
26. Salje J. Plasmid segregation: how to survive as an extra piece of DNA. *Crit Rev Biochem Mol Biol* 2010;**45**:296–317. https://doi.org/10.3109/10409238.2010.494657
27. Ni S, Li B, Tang K *et al.* Conjugative plasmid-encoded toxin–antitoxin system PrpT/PrpA directly controls plasmid copy

number. *Proc Natl Acad Sci USA* 2021;**118**:e2011577118. https://doi.org/10.1073/pnas.2011577118
28. Bustamante P, Iredell JR. The roles of HicBA and a novel toxin–antitoxin-like system, TsxAB, in the stability of IncX4 resistance plasmids in *Escherichia coli*. *J Antimicrob Chemother* 2019;**74**:553–6. https://doi.org/10.1093/jac/dky491
29. McVicker G, Tang CM. Deletion of toxin–antitoxin systems in the evolution of *Shigellasonnei* as a host-adapted pathogen. *Nat Microbiol* 2016;**2**:16204. https://doi.org/10.1038/nmicrobiol.2016.204
30. Cooper TF, Heinemann JA. Postsegregational killing does not increase plasmid stability but acts to mediate the exclusion of competing plasmids. *Proc Natl Acad Sci USA* 2000;**97**:12643–8. https://doi.org/10.1073/pnas.220077897
31. Moritz EM, Hergenrother PJ. Toxin-antitoxin systems are ubiquitous and plasmid-encoded in vancomycin-resistant *enterococci*. *Proc Natl Acad Sci USA* 2007;**104**:311–6. https://doi.org/10.1073/pnas.0601168104
32. Liu YY, Wang Y, Walsh TR *et al.* Emergence of plasmid-mediated colistin resistance mechanism MCR-1 in animals and human beings in China: a microbiological and molecular biological study. *Lancet Infect Dis* 2016;**16**:161–8. https://doi.org/10.1016/S1473-3099(15)00424-7
33. Wang Y, Zhang R, Li J *et al.* Comprehensive resistome analysis reveals the prevalence of NDM and MCR-1 in Chinese poultry production. *Nat Microbiol* 2017;**2**:16260. https://doi.org/10.1038/nmicrobiol.2016.260
34. Liu JH, Liu YY, Shen YB *et al.* Plasmid-mediated colistin-resistance genes: *mcr*. *Trends Microbiol* 2024;**32**:365–78. https://doi.org/10.1016/j.tim.2023.10.006
35. Gao R, Hu Y, Li Z *et al.* Dissemination and mechanism for the MCR-1 colistin resistance. *PLoS Pathog* 2016;**12**:e1005957. https://doi.org/10.1371/journal.ppat.1005957
36. Walsh TR, Wu Y. China bans colistin as a feed additive for animals. *Lancet Infect Dis* 2016;**16**:1102–3. https://doi.org/10.1016/S1473-3099(16)30329-2
37. Wang Q, Sun J, Li J *et al.* Expanding landscapes of the diversified *mcr-1*-bearing plasmid reservoirs. *Microbiome* 2017;**5**:70. https://doi.org/10.1186/s40168-017-0288-0
38. Wang R, van Dorp L, Shaw LP *et al.* The global distribution and spread of the mobilized colistin resistance gene *mcr-1*. *Nat Commun* 2018;**9**:1179. https://doi.org/10.1038/s41467-018-03205-z
39. Chen L, Chavda KD, Al Laham N *et al.* Complete nucleotide sequence of a bla_{KPC}-harboring IncI2 plasmid and its dissemination in New Jersey and New York hospitals. *Antimicrob Agents Chemother* 2013;**57**:5019–25. https://doi.org/10.1128/AAC.01397-13
40. Stokes MO, Abuoun M, Umur S *et al.* Complete sequence of pSAM7, an IncX4 plasmid carrying a novel $bla_{CTX-M-14b}$ transposition unit isolated from *Escherichia coli* and *Enterobacter cloacae* from cattle. *Antimicrob Agents Chemother* 2013;**57**:4590–4. https://doi.org/10.1128/AAC.01157-13
41. Han S, Kim JS, Hong CK *et al.* Identification of an extensively drug-resistant *Escherichia coli* clinical strain harboring *mcr-1* and bla_{NDM-1} in Korea. *J Antibiot* 2020;**73**:852–8. https://doi.org/10.1038/s41429-020-0350-1
42. Shen C, Zhong LL, Yang Y *et al.* Dynamics of *mcr-1* prevalence and *mcr-1*-positive *Escherichia coli* after the cessation of colistin use as a feed additive for animals in China: a prospective cross-sectional and whole genome sequencing-based molecular epidemiological study. *Lancet Microbe* 2020;**1**:e34–43. https://doi.org/10.1016/S2666-5247(20)30005-7
43. Schmartz GP, Hartung A, Hirsch P *et al.* PLSDB: advancing a comprehensive database of bacterial plasmids. *Nucleic Acids Res* 2022;**50**:D273–8. https://doi.org/10.1093/nar/gkab1111
44. Madeira F, Madhusoodanan N, Lee J *et al.* The EMBL-EBI Job Dispatcher sequence analysis tools framework in 2024. *Nucleic Acids Res* 2024;**52**:W521–5. https://doi.org/10.1093/nar/gkae241
45. Robert X, Gouet P. Deciphering key features in protein structures with the new ENDscript server. *Nucleic Acids Res* 2014;**42**:W320–4. https://doi.org/10.1093/nar/gku316
46. Liu X, Li Y, Guo Y *et al.* Physiological function of Rac prophage during biofilm formation and regulation of rac excision in *Escherichia coli* K-12. *Sci Rep* 2015;**5**:16074. https://doi.org/10.1038/srep16074
47. Schägger H. Tricine-SDS–PAGE. *Nat Protoc* 2006;**1**:16–22. https://doi.org/10.1038/nprot.2006.4
48. Karimova G, Pidoux J, Ullmann A *et al.* A bacterial two-hybrid system based on a reconstituted signal transduction pathway. *Proc Natl Acad Sci USA* 1998;**95**:5752–6. https://doi.org/10.1073/pnas.95.10.5752
49. Guo Y, Quiroga C, Chen Q *et al.* RalR (a DNase) and RalA (a small RNA) form a type I toxin–antitoxin system in *Escherichia coli*. *Nucleic Acids Res* 2014;**42**:6448–62. https://doi.org/10.1093/nar/gku279
50. Widdel F. Theory and measurement of bacterial growth. *Di Dalam Grund Mikrobiol* 2007;**4**:1–11.
51. Meinersmann RJ. The biology of IncI2 plasmids shown by whole-plasmid multi-locus sequence typing. *Plasmid* 2019;**106**:102444. https://doi.org/10.1016/j.plasmid.2019.102444
52. Guan J, Chen Y, Goh YX *et al.* TADB 3.0: an updated database of bacterial toxin–antitoxin loci and associated mobile genetic elements. *Nucleic Acids Res* 2024;**52**:D784–90. https://doi.org/10.1093/nar/gkad962
53. Furuya N, Komano T. Mutational analysis of the R64 oriT region: requirement for precise location of the NikA-binding sequence. *J Bacteriol* 1997;**179**:7291–7. https://doi.org/10.1128/jb.179.23.7291-7297.1997
54. d'Aubenton Carafa Y, Brody E, Thermes C. Prediction of rho-independent *Escherichia coli* transcription terminators. A statistical analysis of their RNA stem-loop structures. *J Mol Biol* 1990;**216**:835–58. https://doi.org/10.1016/S0022-2836(99)80005-9
55. Chen YJ, Liu P, Nielsen AA *et al.* Characterization of 582 natural and synthetic terminators and quantification of their design constraints. *Nat Methods* 2013;**10**:659–64. https://doi.org/10.1038/nmeth.2515
56. Turnbull KJ, Gerdes K. HicA toxin of *Escherichia coli* derepresses *hicAB* transcription to selectively produce HicB antitoxin. *Mol Microbiol* 2017;**104**:781–92. https://doi.org/10.1111/mmi.13662
57. Wang X, Kim Y, Hong SH *et al.* Antitoxin MqsA helps mediate the bacterial general stress response. *Nat Chem Biol* 2011;**7**:359–66. https://doi.org/10.1038/nchembio.560
58. Cooper TF, Heinemann JA. Selection for plasmid post-segregational killing depends on multiple infection: evidence for the selection of more virulent parasites through parasite-level competition. *Proc Biol Sci* 2005;**272**:403–10.
59. Cooper TF, Paixao T, Heinemann JA. Within-host competition selects for plasmid-encoded toxin–antitoxin systems. *Proc Biol Sci* 2010;**277**:3149–55.
60. Mhlanga-Mutangadura T, Morlin G, Smith AL *et al.* Evolution of the major pilus gene cluster of *Haemophilusinfluenzae*. *J Bacteriol* 1998;**180**:4693–703. https://doi.org/10.1128/JB.180.17.4693-4703.1998
61. Makarova KS, Grishin NV, Koonin EV. The HicAB cassette, a putative novel, RNA-targeting toxin–antitoxin system in archaea and bacteria. *Bioinformatics* 2006;**22**:2581–4.
62. Jørgensen MG, Pandey DP, Jaskolska M *et al.* HicA of *Escherichia coli* defines a novel family of translation-independent mRNA interferases in bacteria and archaea. *J Bacteriol* 2009;**191**:1191–9. https://doi.org/10.1128/JB.01013-08
63. Mikita N, Cheng I, Fishovitz J *et al.* Processive degradation of unstructured protein by *Escherichia coli* Lon occurs via the slow, sequential delivery of multiple scissile sites followed by rapid and synchronized peptide bond cleavage events. *Biochemistry* 2013;**52**:5629–44. https://doi.org/10.1021/bi4008319

64. Sanchez-Torres V, Hwang HJ, Wood TK. Conformational change as a mechanism for toxin activation in bacterial toxin–antitoxin systems. *J Virol* 2024;**98**:e0151324. https://doi.org/10.1128/jvi.01513-24
65. Gerdes K. Diverse genetic contexts of HicA toxin domains propose a role in anti-phage defense. *mBio* 2024;**15**:e0329323. https://doi.org/10.1128/mbio.03293-23
66. San Millan A, MacLean RC. Fitness costs of plasmids: a limit to plasmid transmission. *Microbiol Spectr* 2017;**5**:mtbp–0016–2017. https://doi.org/10.1128/microbiolspec.MTBP-0016-2017
67. Rodriguez-Beltran J, DelaFuente J, Leon-Sampedro R *et al.* Beyond horizontal gene transfer: the role of plasmids in bacterial evolution. *Nat Rev Micro* 2021;**19**:347–59. https://doi.org/10.1038/s41579-020-00497-1
68. Snesrud E, He S, Chandler M *et al.* A model for transposition of the colistin resistance gene *mcr-1* by IS*Apl1*. *Antimicrob Agents Chemother* 2016;**60**:6973–6. https://doi.org/10.1128/AAC.01457-16
69. Che Y, Yang Y, Xu X *et al.* Conjugative plasmids interact with insertion sequences to shape the horizontal transfer of antimicrobial resistance genes. *Proc Natl Acad Sci USA* 2021;**118**:e2008731118. https://doi.org/10.1073/pnas.2008731118
70. Yi L, Yu K, Gao G *et al.* Successful spread of *mcr-1*-bearing IncX4 plasmids is associated with variant in replication protein of IncX4 plasmids. *J Glob Antimicrob Resist* 2024;**36**:365–70. https://doi.org/10.1016/j.jgar.2024.01.012
71. Yu MK, Fogarty EC, Eren AM. Diverse plasmid systems and their ecology across human gut metagenomes revealed by PlasX and MobMess. *Nat Microbiol* 2024;**9**:830–47. https://doi.org/10.1038/s41564-024-01610-3

Received: October 24, 2024. **Revised:** January 24, 2025. **Editorial Decision:** February 5, 2025. **Accepted:** February 10, 2025